Understanding Biomass Pyrolysis Kinetics: Improved Modeling Based on Comprehensive Thermokinetic Analysis

Departament d'Enginyeria Química
Escola Tècnica Superior d'Enginyeria Industrial de Barcelona
Universitat Politècnica de Catalunya

Understanding Biomass Pyrolysis Kinetics: Improved Modeling Based on Comprehensive Thermokinetic Analysis

Thesis

In partial fulfillment of the requirements for the degree of Doctor
Universitat Politècnica de Catalunya,
directed by Dr. Luis Puigjaner i Corbella and Dr. Enric Velo García,
in Barcelona, November 2006.

Claudia Juliana Gómez Díaz
Chemical Engineer

A mis padres y hermanas.

Summary

Biomass has historically supplied human needs for food, fiber, energy, and structural material. The potential for biomass to supply much larger amounts of useful energy with reduced environmental impacts compared to fossil fuels has stimulated substantial research and development of systems for handling, processing, and converting biomass to heat, electricity, solid, liquid and gaseous fuels, and other chemicals and products. Greater use of biomass has also been motivated by improvements experienced in local and global environmental quality. Pyrolysis and other thermochemical conversion processes offer an important opportunity for the utilization of biomass and waste. The increasing dependence on imported oil as well as the urgency to reduce Greenhouse emissions abounds in justifying an energy policy that carefully considers the role of renewable sources as energy carrier.

Although numerous projects have been promoted, pyrolysis commercialization is progressing at a low pace not only in Europe but also globally. Major efforts on researching are needed in order to maximize the advantages and minimize the disadvantages of this technology. The upsurge of interest in simulation and optimization of suitable reactors for thermochemical processes requires appropriate models that contemplate different operational conditions and varied feed stocks and helping to achieve a better understanding of the reactions in the corresponding processes. In this sense, a better knowledge of the kinetics concerning to the thermal decomposition of the lignocellulosic materials is required.

The abundant research literature on the field of biomass pyrolysis kinetics still leaves key issues unsolved. The exploitation of the information provided by thermogravimetry, a relatively low priced, simple technique suitable for studying several reactions of interest in biomass conversion and combustion, requires the establishing of appropriate models and evaluation strategies for the various biomass materials. The kinetic description of experiments measured at different conditions by exactly the same reaction kinetics is criticized due to some small, but inevitable systematic errors that depend on the experimental conditions. Practical models that predict the evolution of specific products of interest are still expected in the literature. Part of the chemical phenomena referred to the secondary interactions between the primary pyrolysis products has been traditionally avoided when modeling the pyrolytic process.

Summary

The increased exploitation of herbaceous crops, in addition to the large quantity of woody residues that still remains largely unused, currently ask for a better description of the influence of the heterogeneities on biomass thermolysis.

This thesis addresses all these issues in the context of fundamental research. The thermal behavior of biomass materials representative of carpentry residues (pine and beech), and an energy plantation (thistle) is studied by different thermoanalytical techniques, within the range of slow pyrolysis, including various pretreatments to eliminate inorganic matter and extractives. The first contribution aims at deeply observing the extent of systematic errors associated to the experimental part of the thermogravimetric studies. The thermal behavior of the same feedstock in different original equipments, under roughly equivalent experimental conditions, is statistically studied. Then, various approaches based on first and nth-order partial reactions in the summative model of pseudocomponents are employed in order to determine the best kinetic parameters that describe the experiments both at linear and stepwise heating programs and for experiments coming from different sources. A common set of activation energies, coming from the evaluation of water-washed samples, is applied for the kinetic description of all the types of experiments performed along this thesis.

Mass spectrometry, simultaneously coupled to thermogravimetry, is used as the volatile product analysis technique. A chemometric tool is applied to help in elucidating the specific influence of the macromolecular composition of the samples on the thermal decomposition and on the product distribution. Making use of calibration data, we estimate the individual production of the major volatile species from slow pyrolysis. Then, an approximation of the vapor-phase product distribution is added to the kinetic mechanism.

We are also interested in the study of the secondary biomass pyrolysis. Differential scanning calorimetry is the technique used to observe the information traced by the heat of pyrolysis on the primary and secondary decomposition. Additionally, we analyze results from a Fourier transform infrared spectroscopy device coupled with thermogravimetry, in order to assess the secondary phenomena by considering the evolution profiles of the volatile products, as well. Finally, we test the ability of the best kinetic approach, from the previous kinetic analysis, to describe the global mass loss under conditions that clearly favor secondary vapor-solid interactions too.

Overall, this research work represents a comprehensive and thorough thermokinetic study of biomass pyrolysis that approaches the thermal behavior by recognizing the connections between different chemical phenomena making up the pyrolytic process. The kinetic proposal, finally built up in this thesis, is a contribution for understanding the process as a whole. Additionally, it can be considered as a first step toward its extension to practical applications, where additional chemical and transport phenomena need to be incorporated.

Resumen

La biomasa, a lo largo de la historia de la humanidad, ha satisfecho necesidades de alimento, fibra, energía y material estructural. Su potencial como recurso de energía útil, con reducido impacto ambiental comparado con los combustibles fósiles, ha estimulado la investigación y desarrollo en las áreas de manejo y procesamiento de biomasa para la producción de calor, electricidad, combustibles sólidos, líquidos y gaseosos, así como para la producción de productos químicos en general. La necesidad de mejoramiento de la calidad ambiental a nivel local y global también ha motivado un mayor y mejor uso de la biomasa. La pirólisis, junto con otros procesos de conversión termoquímica, representa una opción interesante para la revalorización de la biomasa y los residuos orgánicos. Los altos índices de importación de combustibles a nivel mundial, así como la urgente necesidad de reducir la emisión de gases de efecto invernadero, son parte de las razones por las cuales las políticas energéticas mundiales deben considerar el rol de los recursos renovables como fuente de energía.

A pesar de los numerosos proyectos relacionados con el tema, que se han venido llevando a cabo por varias décadas, el desarrollo de la tecnología de pirólisis, tanto en Europa como a nivel mundial, no ha avanzado a un buen ritmo. Aún se requiere mayor soporte a la investigación para maximizar las ventajas y minimizar las desventajas de esta tecnología. El creciente interés en la simulación y optimización de reactores para procesamiento termoquímico debería estar ligado a la consideración de modelos más apropiados, que tengan en cuenta diferentes condiciones de operación y variedad de materia prima, y que a la vez sirvan como herramienta para una mejor comprensión de las reacciones químicas que estos procesos conllevan. Este es el marco para introducir la necesidad de un mejor entendimiento de la cinética de descomposición térmica de materiales lignocelulósicos, lo que constituye el objeto de esta tesis.

En el campo de la cinética de la pirólisis de biomasa también se han desarrollado numerosos trabajos de investigación que no acaban de resolver aspectos básicos del proceso. La termogravimetría es la técnica común que se emplea en este tipo de investigaciones. Es una técnica sencilla, de bajo coste, y de alta aplicación para el estudio de varias reacciones de interés en procesos de devolatilización y combustión. Sin embargo, el análisis de resultados termogravimétricos aún requiere el establecimiento de modelos y estrategias de evaluación más apropiadas para los diferentes tipos de bio-

masa. El uso de una ley cinética común para la descripción de experimentos llevados a cabo a diferentes condiciones de operación es criticado por la inevitable intromisión de errores sistemáticos debidos a las condiciones experimentales. Modelos prácticos, que predigan la evolución de productos específicos de interés, no son comunes en la literatura. Por otro lado, existe una parte del fenómeno químico, relacionada con las interacciones secundarias entre productos primarios de pirólisis, que tradicionalmente se deja a un lado en el modelado del proceso. La creciente explotación de cultivos para el aprovechamiento energético, así como la extensa cantidad de residuos de madera que aún se encuentran sin utilizar, requieren una mejor descripción de la influencia del carácter heterogéneo de estos materiales en la termólisis de biomasa.

Esta tesis trata todos estos aspectos desde el punto de vista de la investigación fundamental. Se estudia el comportamiento térmico de biomasas representativas de los residuos de carpintería (madera de pino y haya) y de un cultivo energético (cardo borriquero) por medio de diferentes técnicas termoanalíticas, en el régimen de pirólisis lenta (slow pyrolysis), incluyendo varios pretratamientos de la biomasa para eliminar materia inorgánica y componente extractivo. La primera contribución de esta tesis corresponde a un estudio exhaustivo del efecto de los errores sistemáticos asociados a la experimentación en termogravimetría. El comportamiento térmico de un mismo material es observado en diferentes termobalanzas, bajo condiciones que se consideran equivalentes entre diferentes equipos, y los resultados son analizados estadísticamente. Consecutivamente, para la descripción de la pérdida global de masa, se estudian diferentes aproximaciones cinéticas basadas en reacciones parciales de primer y otros órdenes, por el modelo de pseudocomponentes. Se trata de determinar un conjunto común de parámetros cinéticos que describan satisfactoriamente experimentos provenientes de diversas termobalanzas y bajo diferentes regímenes de calentamiento: lineal y en escalera (aplicación sucesiva de rampas y periodos isotérmicos de calentamiento). Un conjunto común de energías de activación, resultado de la evaluación cinética de muestras pretratadas (lavadas con agua a 80 °C), es aplicado en la descripción cinética de todos los tipos de experimentos llevados a cabo a lo largo de la tesis.

Espectrometría de masas, acoplada simultáneamente a la termogravimetría, es la técnica empleada para el análisis de los productos volátiles. Se aplica una herramienta estadística para analizar la influencia de la composición de las muestras en la descomposición térmica global y en la distribución de productos. Por medio de datos de calibración se estima la producción individual de los principales productos volátiles de la pirólisis. Consecutivamente, se incluye una aproximación de la evolución de dichos productos en el modelo cinético global.

El estudio de las reacciones secundarias de pirólisis ha sido también parte importante en esta tesis. A través de la calorimetría diferencial se estudia el calor de reacción de la descomposición primaria y secundaria. Adicionalmente, se analizan los resultados provenientes de un estudio de espectroscopía infrarroja acoplada a termogravimetría, con el objeto de investigar la descomposición secundaria mediante la observación de los perfiles de evolución de los productos volátiles. Finalmente, se prueba y optimiza el desempeño del modelo cinético global para describir la descomposición térmica de muestras bajo condiciones que claramente favorecen la descomposición

secundaria.

En conjunto, este trabajo de investigación representa un estudio termocinético exhaustivo y profundo de la pirólisis de biomasa. La descomposición térmica se aborda a través de la observación de la interconexión entre los diferentes fenómenos químicos que conforman el proceso. La propuesta de aproximación cinética, que se constituye a lo largo de la tesis, contribuye al entendimiento del proceso como un todo. Puede ser también considerada como un primer paso hacia la aplicación de los modelos cinéticos de pirólisis a otros estudios, requiriéndose la incorporación adicional de fenómenos de transporte y otras consideraciones para su posterior aplicación.

Acknowledgments

A long time ago, someone told me that the Acknowledgments were the most important part to write in a thesis. Maybe that person was right... This is like a window to show the human side of all this work, and a fair opportunity to say everybody involved in this process THANKS. I am talking about a process that not only implied an academic and educational perspective, but also a personal growing. Mentioning all people who deserve my gratitude without leaving someone out is quite a difficult task, but I will try to do my best.

First, I want to express my gratitude to my family, in Colombia, to whom I also want to dedicate this work. Thanks to their support and confidence I had enough grip to move to Barcelona and start my PhD studies. I really appreciate their patience and strength to afford the sacrifice that the distance implies. Thanks to this important decision, I have had the opportunity to live one of the most exciting and enriching experiences in my life. Without hesitation, this is what I appreciate the most from this period of my life.

I acknowledge the financial support received from the Ministerio de Educación y Ciencia (FPU research grant and project PPQ2000-0300-P4-2) and the European Community (project RFC-CR-04006).

I would also like to express my gratitude to my advisers Lluis Puigjaner and Enric Velo, for the opportunities given and their support at decisive moments of my studies. I am also in debt with all my colleagues from the CEPIMA group, who have contributed to create a very pleasant atmosphere at work. I would like to mention Fernando, Anna, Pepe, Gonzalo, Estanislao, Eloy and Francisco for their unconditional help and friendship. Thanks also to Joan Manyà, now at the University of Zaragoza, for his ideas an initial support.

The results of this thesis would not have been possible without the professional contribution of the international research groups that kindly collaborated with us in our investigations. I wish to dedicate special words of gratitude to Gábor Várhegyi, Erika Mészáros and Emma Jakab from the Hungarian Academy of Sciences. The valuable scientific support that I have received from all them has been crucial for the development of my thesis. Besides, I wish to thank Valerio Cozzani and Federica Barontini, from the University of Pisa, for their valuable suggestions, unconditional

help and confidence posed in my work.

Finally, there is a group of people behind this thesis and research environment that I would like to mention. They have somehow "suffered" this period with me and have constituted my big family in Barcelona. Especially, I would like to express my affection to Laura and Martha, my "moms" and fundamental support to my life here; the loving Silvina and Sebastián; Joan, Laura, Carles, Cesca, Alfredo and Xavier, who have been much more than my choir mates; Pep and the other "Cantiga" choir members, who have allowed me to dream with music. I want to say thanks to all these people for having contributed to make my life in Barcelona worthy.

Agradecimientos

Hace algún tiempo alguien me dijo que los agradecimientos eran la parte más importante de una tesis... Quizás esa persona tenía razón. Son como una ventana donde se puede ver la parte más humana detrás de todo este trabajo, y la oportunidad precisa para decir a todas las personas que de una u otra manera han estado involucradas en este proceso, GRACIAS. Estoy hablando de un proceso no solamente desde el ámbito académico e intelectual, sino también un crecimiento personal. Es muy difícil pretender mencionar a todos a los que debería agradecer sin dejarme alguno fuera, pero intentaré hacer lo mejor posible.

Principalmente, quiero expresar mi gratitud a mi familia, en Colombia, a quienes dedico este trabajo. Gracias a su apoyo y a su confianza tuve la fuerza necesaria para viajar a Barcelona y comenzar mis estudios de doctorado. Realmente aprecio la paciencia y la fuerza que han tenido para afrontar el sacrificio que implica la distancia. Gracias a esta decisión tan importante, he tenido la oportunidad de vivir una de las experiencias más emocionantes y enriquecedoras de mi vida. Sin duda, esto es de lo que más valoro durante este periodo de mis estudios.

Agradezco el apoyo económico del Ministerio de Educación y Ciencia (beca FPU y proyecto PPQ2000-0300-P4-2) y de la Comunidad Europea (proyecto RFC-CR-04006).

Quiero agradecer a mis tutores, Lluis Puigjaner y Enric Velo, por las oportunidades que me brindaron y por su apoyo en momentos decisivos de mis estudios. También estoy en deuda con mis compañeros del grupo CEPIMA, quienes han contribuido a crear un ambiente realmente agradable en el trabajo diario. Especialmente me gustaría mencionar a Fernando, Anna, Pepe, Gonzalo, Estanislao, Eloy y Francisco por su ayuda incondicional y su amistad. Gracias también a Joan Manyà, ahora en la Universidad de Zaragoza, por sus ideas y su apoyo en los comienzos de este trabajo.

Los resultados de esta tesis no habrían sido posibles sin la ayuda de los grupos de investigación que amablemente colaboraron con nosotros. Quiero dedicarle palabras especiales de agradecimiento a Gábor Várhegyi, Erika Mészáros y Emma Jakab de la Academia Húngara de Ciencias. Su valioso apoyo científico fue crucial en el desarrollo de esta tesis. Además, quiero agradecer a Valerio Cozzani y a Federica Barontini, de la Universidad de Pisa, por sus valiosas sugerencias, su ayuda incondicional y la

confianza puesta en mi trabajo.

Finalmente, hay un grupo de personas detrás de esta tesis y del ambiente de investigación que me gustaría mencionar. Ellos de alguna manera han "padecido" este periodo de tiempo conmigo y han sido como mi gran familia en Barcelona. Especialmente quiero expresar mi afecto a Laura y a Martha, mis "mamis" y mi soporte fundamental en este ciudad; a los amorosos Silvina y Sebastián; a Joan, Laura, Carles, Cesca, Alfredo y Xavier quienes han sido mucho más que mis compañeros de coral; a Pep y el resto de miembros de la coral Cantiga, quienes me han permitido soñar con la música. Quiero decirles gracias a todos ellos, por haber hecho que mi vida en Barcelona valiera la pena.

Contents

Chapter

ONE

Introduction

This chapter includes a brief description of chemical characteristics and energy potential of biomasses, as well as an overview of the main thermochemical process for biomass conversion. Since we will be focused on pyrolysis, this chapter ends with the role of this technology as an alternative for waste upgrading, particularly within the scope of fundamental research. The intention is to place the reader within the framework of this thesis. The last section presents the outline of the entire document so as to help the reader in following the exposition.

1.1 Types of Biomass. General characteristics

Biomass can generally be defined as any hydrocarbon material. Some biomass types also carry significant proportions of inorganic species. Sources include various natural and derived materials, such as woody and herbaceous species, woody wastes (e.g. from forest thinning and harvesting, timber production and carpentry residues), agricultural and industrial residues, waste paper, municipal solid waste, sawdust, grass, waste from food processing, animal wastes, aquatic plants and industrial and energy crops grown for biomass. For political purposes, some other materials (such as tires, manufactured from either synthetic or natural rubbers) may be included under the general definition of biomass even though the material is not strictly biogenic (Klass, 1998; Hall and Overend, 1987).

Agricultural and forest residues are produced as secondary products of the primary commodity production system. Special attention is given to the production of energy crops. It refers to dedicated crops produced at relatively high photosynthetic efficiency, or high carbohydrate content and other hydrocarbon materials, so as to be used as energy source. A number of most commonly considered agricultural and woody residues, as well as energy crops are listed in Table 1.1.

The end use for biomasses can influence the management and cultural inputs and practices employed to optimize the production system. Herbaceous species, for example, generally contain more ash than wood, and the ash is higher in alkali metals

Table 1.1: Selected biomass materials.

Woody species - biomass/fiber/pulp
Alder (*Alnus spp.*)
Beech (*Fagus sylvatica*)
Birch (*Onopordum nervosum*)
Black locust (*Robinia pseudoacacia*)
Eucalyptus (*Eucalyptus spp.*)
Eastern cottonwood (*Populus deltoides*
Fir (*Douglas fir, White fir*)
Maple (*Silver maple*)
Oak (*Quercus coccifera, Quercus ilex*)
Pine (*Pinus pinea, Pinus halepensis, Pinus brutia, Pinus pinaster*)
Poplar (*Populus spp.*)
Spruce (*Picea glauca*)
Willow (*Salix spp.*)
Herbaceous species: biomass/fiber/energy grain
Arundo donax
Jose Tall wheatgrass (*Agropyrum elongata*)
Miscanthus (*Miscanthus spp.*)
Napier grass/Banagrass (*Pennisetum purpureum*)
Spanish thistle or Cardoon (*Cynara cardunculus*)
Spring barley (*Hordeum vulgare*)
Switchgrass (*Panicum virgatum L.*)
Triticale (*Triticosecale*)
Winter wheat (*Triticum aestivum*)
Herbaceous species: sugar/starch/biomass
Buffalo gourd (*Curcurbita foetidissima*)
Cassava (*Manihot esculenta*)
Jerusalem artichoke (*Helianthus tuberosus*)
Sugar/Energy cane (*Saccharum spp.*)
Sugar/Fodder beet (*Beta vulgaris*)
Sweet sorghum (*Sorghum bicolor*)
Other agricultural residues
Almond shells
Corn stalk
Grape residues
Nutshells
Olive husks and stones
Rice husks

and silica. The latter combine at high temperature in combustion systems to form slags and deposits that increase maintenance costs.

1.2 Structure, composition, and properties of biomass

Understanding of the chemical structure and major organic components in biomass is extremely important in the development of processes for producing derived fuels and chemicals. Biomass has a complex chemical composition, and both organic and inorganic constituents are important to the handling and conversion processes. The dominant structural compounds making up plant biomasses are cellulose (C_6 polymers), hemicellulose (predominantly C_5 polymers but including C_6 species) and lignins. Organic compounds in biomass also include extractives, non-structural compounds mostly soluble in water and/or various organic solvents (fatty acids, lipids, terpenoids, phenolic compounds, glycosides, proteins, triglycerides, terpenes, waxes, cutin, suberin, flavonoids, betalains, alkaloids). Plants accumulate inorganic materials (ash), sometimes in concentrations exceeding those of hemicellulose or lignin. The concentration of the ash arising from these inorganics changes from less than 1% in softwoods to 15% in herbaceous biomass and agricultural residues (Yaman, 2004).

Cellulose is a linear crystalline polysaccharide, with general formula $(C_6H_{10}O_5)_n$. It serves as the framework substance, making up 40-50% of wood. The polymer is formed from repeating units of cellobiose, a disaccharide of β-linked glucose moieties (Figure 1.1). Hemicelluloses are matrix substances between cellulose microfibrils. They are polysaccharides of variable composition containing both five (including xylose and arabinose) and six carbon monosaccharide units (including galactose, glucose, and mannose). Hemicelluloses constitute 20 to 30% of wood and other biomasses, generally with higher concentrations in hardwoods than softwoods. Partial structures for the primary forms of hemicellulose in hardwood and softwood are shown in Figure 1.2. The most abundant monomeric unit of hemicelluloses is xylan.

The lignins are highly branched, substituted, mononuclear polymers of phenylpropane units, derived from coniferyl, sinapyl, and p-coumaryl alcohols. They are often bounding to adjacent cellulose fibers to form a lignocellulosic complex. The structure varies among different plants. Softwood lignin is composed principally of guaiacyl units stemming from the precursor trans-coniferyl alcohol. Hardwood lignin is composed mostly of guaiacyl and syringyl units derived from trans-coniferyl and trans-sinapyl alcohols. Grass lignin contains p-hydroxyphenyl units deriving from trans-p-coumaryl alcohol. Almost all plants contain all three guaiacyl, syringyl, and p-hydroxyphenyl units in lignin. A partial structure of softwood lignin is shown in Figure 1.3. The lignin contents on a dry basis generally range from 10% to 40% by weight in various herbaceous species (Yaman, 2004).

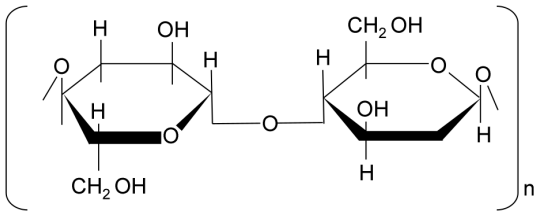

Figure 1.1: Cellobiose, the repeating unit of cellulose (source: Salisbury and Ross (1992)).

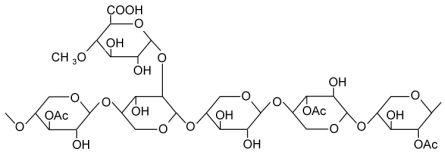

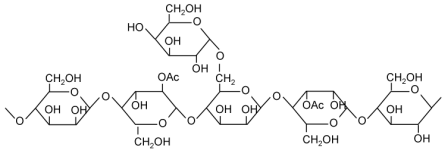

Figure 1.2: Partial structures of the principal hemicelluloses in wood (source: Salisbury and Ross (1992)): O-acetyl-4-O-methylglucuronoxylan from hardwood (A) and O-acetyl-galactoglucomannan from softwood (B). Ac=acetyl group.

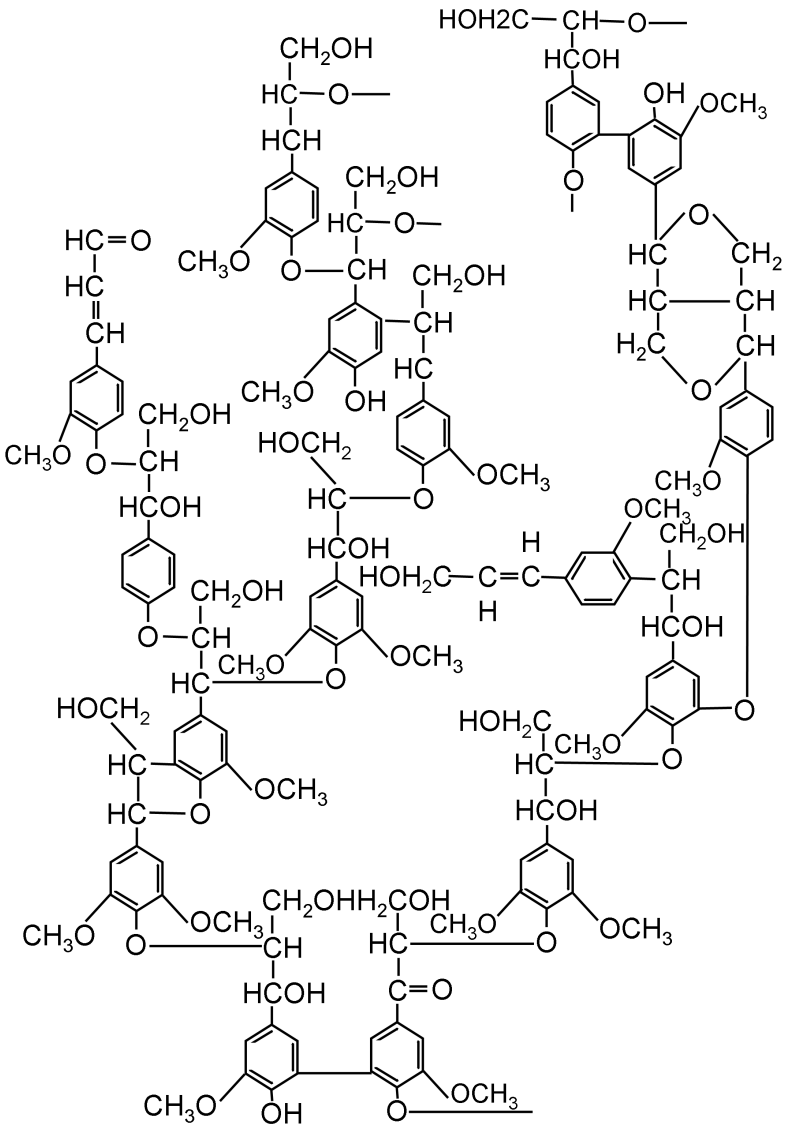

Figure 1.3: Partial lignin structure of softwood (source: Salisbury and Ross (1992)).

1.3 Biomass thermochemical conversion

Figure 1.4 illustrates a few of the numerous possible pathways for generating energy and products from biomass resources. Three principal routes exist for converting biomass: 1) thermochemical, 2) biochemical, and 3) physicochemical. In practice, combinations of two or more of these routes may be used. Thermochemical conversion includes combustion, thermal gasification, and pyrolysis along with a number of variants involving microwave, plasma arc, supercritical fluid, and other processing techniques. Products include heat, fuel gases, liquids, and solids. Biochemical and physicochemical processes are in general more intended to upgrade biomass components and produce higher value products. Thermochemical routes can also be used in this case, as in the indirect production of methanol via gasification. The conversion strategies are integrally coupled to the properties of the biomass. In many cases, the properties of the biomass necessary for engineering design have not been properly characterized prior to commercial implementation of a technology.

Figure 1.4: Biomass processing options (adapted from Klass (1998); Hall and Overend (1987)).

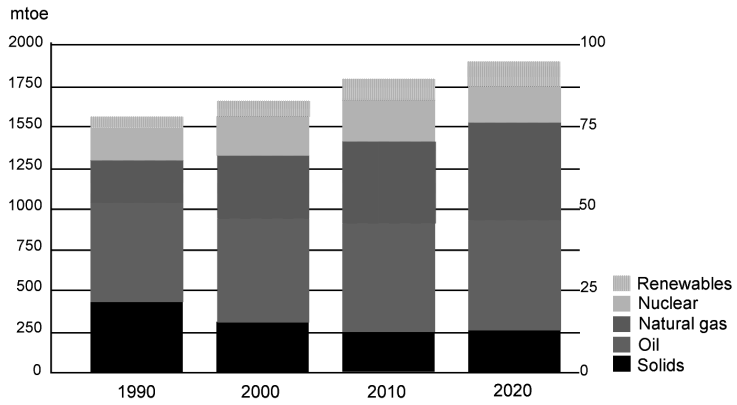

Figure 1.5: Total EU energy consumption by fuel and energy intensity 1990 2020 (source: Green Paper on energy efficiency, 2005, *http://europa.eu.int.*).

1.4 Energy potential of biomass residues

According to the recent Commission's Green Paper on energy efficiency[1], current energy demand in the EU, estimated about 1725 Mtoe (Megatons of oil equivalent) of energy per year, is covered around 80% by fossil fuel, of which over 40% are oil. The contribution of renewable energies remains relatively low, at 6% in 2000, although a share of 10% of the total consumption is expected by 2010 (See Figure 1.5). Burning fossil fuels causes greenhouse gas emissions. CO_2 emissions could, if prevailing trends persist, actually exceed 1990 levels by 14% by 2030. An additional problem for the European Union, mainly due to the continued use of oil, is its degree of import dependency in energy. It has increased from around 40% in 1985 to around 50% today. It is expected to continue rising, possibly reaching 70% in the next 20 years if appropriate measures are not taken (Maniatis et al., 2002).

It is obvious that a robust energy policy has to address this unsatisfactory situation and envisage reversing this trend. Any such a policy has to carefully examine the role of renewable energy sources. In this respect the European Commission has increased the support to programs in the fields of energy efficiency and renewable energy sources. The current tendency is oriented to support research and demonstration activities, in connection with other regulatory and economy-based measures, so as to efficiently increase the share of renewable energies.

Figure 1.6 shows the current contribution of the various renewable energy sources

[1]Green Paper on energy efficiency, 13 December 2005, <*http://europa.eu.int*>.

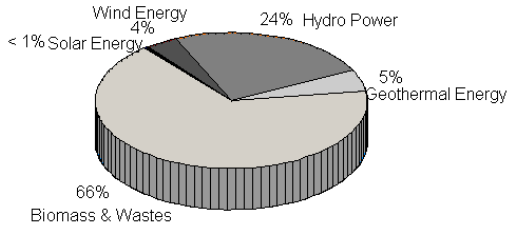

Figure 1.6: 2003 Renewable energy primary production. Contribution from biomass considered as the heat content of the produced biofuels or biogas plus the heat produced after combustion during incineration of renewable wastes (source: Eurostat *http://epp.eurostat.cec.eu.int.*).

to the Union's energy mix. It is manifested that bioenergy (energy from biomass and waste) has the highest contribution amongst all renewable materials. For several reasons bioenergy is globally recognized as the renewable resource that will make the most significant contribution for sustainable energy in the near to medium term (Maniatis et al., 2002). This is the only renewable that can directly replace fossil fuel based energy. The use of biomass as fuel in substitution of fossil resources results in low sulphur dioxide emissions and almost no net atmospheric carbon emissions, and hence serves to mitigate greenhouse gas and global climate change impacts (Kaltschmitt and Dinkelbach, 1997). Besides, upgrading of biomass represents an attractive way of use of agricultural and forestry residues that could renovate rural economies. Biomass crops can in general be used for restoration of degraded or deforested lands, and for economic and environmental reasons are frequently proposed for planting in marginal areas (Berndesa et al., 2003). Biomass production also serves to store solar energy, thus allowing continuous power generation.

However, the current use of renewable sources for energy is limited to an extent, which is considerably lower than their potential. In nearly all of the EU-countries less than 50% of the available biomass resources are currently used. In most countries, the share is even significantly lower. This is mainly due to relatively high costs of the technologies of upgrading. The investment costs can be twice as high compared to fossil-fired plants (the low energy density requires larger plant sizes, the wide variety of fuel characteristics and the objective to achieve a clean combustion require higher efforts in conversion and cleanup technology). There is also a high effort necessary for transportation and storage of biofuels because of the low energy density. Furthermore,

a reliable market for biofuels has not yet been established that ensures availability of biofuels for customers (Maniatis et al., 2002).

There is a public demand for an use of biomass on a large scale above the current level. This can only be carried out, if biomass is processed in a way that makes this energy carrier fit into the European energy system much better on the one hand and achieve a higher value and hence higher prices on the other hand. Modernized bioenergy systems are suggested to be important contributors to future sustainable energy systems and to sustainable development in industrialized countries as well as in developing countries (Berndesa et al., 2003).

1.5 Present challenges of thermochemical technologies

1.5.1 Combustion

Historically, and still so today, the most widely applied conversion method for biomass is combustion. The chemical energy of the fuel is converted via combustion into heat energy, which is useful in and of itself, and which may be transformed by heat engines into mechanical and electrical energy. Direct combustion of biomass is not favored by too high content of moisture, and lower density than that of coal, leading to important economic limitations. The energy efficiency associated to the process is mostly lower than that obtained from a combined cycle gasification plant.

1.5.2 Gasification

Gasification is a partial thermal oxidization, which results in a high proportion of gaseous products (carbon dioxide, water, carbon monoxide, hydrogen, gaseous hydrocarbons), small quantities of char (solid product), ash and condensable compounds (tars and oils). Steam, in addition to air or oxygen, are supplied to the reaction as oxidizing agents. Reaction conditions can be varied to maximize the production of fuel gases, fuel liquids, or charcoal. The term gasification is applied to processes that are optimized for fuel gas production (principally CO, H_2, and light hydrocarbons).

There is renewed attention to gasification due to the possibility to produce synthesis gas and subsequently liquid biofuels or hydrogen. The eventual markets for such bio-products are enormous on a global scale (Maniatis et al., 2002). However, there are still two main problems that hinder the reliable and trouble free operation of this technology: a) a thorough systems approach to a gasification facility that will address all individual sub-systems as well as their interaction as a whole and b) the gas cleaning with the main problem the efficient and economically viable tar elimination. Gasification is characterized by a continuous and constant operation of all subsystems from the material feeding to the generation of power and/or heat, and unless all subsystems operate efficiently the gasification plant in rendered inoperable. Indeed areas such as constant feeding, fouling of heat exchange surfaces, tar elimination, wastewater treatment and disposal of effluents and emissions of NOx continue

presenting barriers that trouble free operation.

1.5.3 Pyrolysis

Pyrolysis of biomass can be described as the direct thermal decomposition of the material in the absence of oxygen to obtain an array of solid, liquid and gas products. Conventional pyrolysis consists of the slow, irreversible, thermal decomposition of the organic components in biomass. Slow pyrolysis has traditionally been used for the production of charcoal. Short residence time pyrolysis (fast, flash, rapid, ultrapyrolysis) of biomass at moderate temperatures has generally been used to obtain high yield of liquid products. Fast pyrolysis is characterized by high heating rates and rapid quenching of the liquid products to terminate the secondary conversion of the products (Yaman, 2004).

Pyrolysis technologies have only been developed for the last 20 years compared to more than 200 years for gasification, and more than 2000 years for combustion. As the technologies are scaled up to commercial size, a number of technical issues will have to be resolved including provision of process heat; heat transfer; hydrodynamics (for fluid bed systems); maintenance of yields; separation of char; biomass preparation; scale-up; feeding; back-mixing in fluid bed systems; control of secondary reactions; and product quality definition, monitoring and control. Pyrolysis should be also viewed as complementary to gasification as a liquid is produced that can be stored and transported to the point of use and can be used intermittently as well as continuously. Gas from gasification cannot be economically stored or transported, so it is better suited to base load applications (Bridgwater, 2002).

A wide range of applications have been investigated and successfully demonstrated as feasible from biomass pyrolysis. The focus of most research and development to date has been on energy applications due to the driving force of political commitments to reduce green house emissions. Apart from the usage as fuel, the products of thermochemical processes can be used in particular fields. For instance, the liquids obtained from pyrolysis contain many chemical compounds that can be used as feedstock for synthesis of fine chemicals, adhesives, fertilizers, resins, production of hydrogen, food flavors, emission control reagents, hydroxyacetaldehyde, levoglucosan and some other commodities (Bridgwater, 2002).

The solid products from pyrolysis contain char, ash and unchanged biomass material. The pyrolysis conditions determine the chemical composition of those products. As a renewable fuel, charcoal has many attractive features: it contains virtually no sulfur or mercury and is low in nitrogen and ash; it is highly reactive yet easy to store and handle. Carbonized charcoal can be a good adsorbent with a large surface area and a semimetal with an electrical resistivity comparable to that of graphite. Recent advances in knowledge about the production and properties of charcoal presage its expanded use as a renewable fuel, reductant, adsorbent, and soil amendment (Yaman, 2004; Antal and Grønli, 2003). Heating values of the chars obtained from pyrolysis are comparable with those of lignite and coke, and the heating values of liquids are comparable with those of oxygenated fuels, such as CH_3OH and C_2H_5OH, which are 40 - 50% of that for hydrocarbon fuels. The heating value of gases is comparable

with those of producer gas or coal gas and is much lower than that of natural gas. The heating values of the products are functions of the initial composition of the biomass (Yaman, 2004). The use of biomass for materials can be expanded to new applications. For example, biomass can be used further as a carbon neutral alternative for coal and coke in the iron and steel industry. Biomass can also be used as a renewable carbon feedstock in the production of synthetic organic materials such as basic chemicals, plastics, paint and solvents (Hoogwijka et al., 2003).

1.6 Thesis scope and outline

Fundamental research is still one of the challenges and opportunities for successful development of pyrolysis technologies. As the technology and applications for the products have developed, so has knowledge and awareness of the technical and economical challenges to be addressed. Table 1.2 points out the role that fundamental research can play in aiding successful commercialization of the pyrolysis products, which is within the scope of this thesis.

In general, this work addresses thermokinetic approaches for the description of biomass pyrolysis. These approaches come from the application of different thermoanalytical techniques along the chapters of this thesis.

After the current introductory view, Chapter 2 consists in a bibliography review that addresses to some extent the most significant issues around pyrolysis kinetics and product distribution. It also includes the main trends and challenges which are useful to draw the objectives of this thesis. Detailed review on specific concepts can be found in those chapters where they are mentioned.

The main contributions of this work are essentially included in Chapters 3 to 6. Every chapter include a selection of resulting figures and tables. Some of them have been already published or are part of papers submitted for publication. Citations to those publications (which are listed in the Appendix A) are employed whenever it is applicable along the text.

Chapter 3 exposes the experimental procedure followed in the thermogravimetric studies carried out along this work, as well as the entire characterization of the experimental results. Specific experimental systems corresponding to the additional techniques (different from thermogravimetry) used in this thesis will be detailed in those chapters where they are mentioned.

Chapter 4 introduces the kinetic approaches exposed in this thesis and explains the mathematical procedures for the reliable determination of the kinetic parameters that describe the primary pyrolysis process. Series of validations of these parameters will be presented, for different experimental conditions.

Chapters 5 and 6 present the results of the thermoanalytical studies that were coupled to thermogravimetry (i.e., differential scanning calorimetry, Fourier transform infrared spectroscopy and mass spectrometry). These results will help in the integration of product distribution and secondary decomposition to the kinetic approach.

Chapter 7 discusses additional applications of the pyrolysis kinetic approaches and

Table 1.2: Challenges and opportunities for the successful development of pyrolysis technologies within the scope of fundamental research. Adapted from Bridgwater (2002).

	Challenges	**Opportunities**
Feed production	Feed selection Feed characterisation	Improve feed specificacions and stablish relationships between feed and product characteristics.
	Challenges	**Opportunities**
Reactor and reaction	Heat transfer rates and heat transfer area	Fundamental research to improve design methods and modelling.
	Holocellulose and lignin cracking	Fundamental research into primary and secondary reactions, leading to improved reactor design and process design. Process improvement and optimisation.
	Secondary reactions	Fundamental research into primary and secondary reactions, leading to improved reactor design and process design. Process improvement and optimisation.
Products quality	Stability	Fundamental research to understand stability and relate it to process parameters, technology and feedstock. Improve process and process control.
	Yield	Fundamental research to optimise the production of an specific product of interest.
	Challenges	**Opportunities**
Scale up	Design and optimization	Successfully apply the results from laboratory, pilot plant and demonstration facilities. Use of modelling. Connection to some other thermochemical conversion processes like gasification.

addresses future work. Finally, Chapter 8 summarizes the thesis contribution.

Chapter

TWO

State of the art and literature review

The upsurge of interest in simulation and optimization of the reactors for thermochemical processes requires appropriate models that help to achieve a better understanding of the reactions in the corresponding processes. In this sense, a better knowledge of the kinetics concerning to the thermal decomposition of the lignocellulosic materials is required.

In the present chapter, the most significant contributions on the literature of pyrolysis kinetics and product distribution are presented. It starts with a summary of the main concepts related to pyrolysis of lignocellulosic materials. The review includes studies concerning primary and secondary decomposition, as well as some other key issues, i.e. heat of reaction, product distribution and data analysis. Following the trends and challenges found from the analysis of the current approaches, the specific objectives of the thesis are formulated.

2.1 Biomass pyrolysis: An overview

Pyrolysis of biomass appears within the most promising conversion routes of waste upgrading, on the short to long term. This process shows favorable technical and system technical characteristics, with very promising feedstock availability and products applications. Also the most important system aspects (like cost reduction potential, integration into the energy system, environmental benefits) are advantageous.

When lignocellulosic materials are exposed to inert high-temperature atmosphere, they degrade into hundreds of species generally classified, from the practical point of view, in char (the rich non-volatiles solid residue) and volatile products (low molecular weight gaseous species, in addition to all condensible, aqueous and high molecular weight organic compounds or tars). These chemical degradations are cataloged as primary reactions, mainly endothermic. Volatile products of primary biomass degradation are transported toward the heated surface of the solid (high temperature pyrolysis zone), and they may undergo further secondary reactions occurring either homogeneously in the gas phase or heterogeneously on the surface of the char. The

whole phenomena implies exceedingly complex pyrolysis chemistry, because series of dehydration, depolymerisation, and cracking reactions are developed by effect of the high temperature and the solid-vapour interaction.

Depending on the pyrolysis temperature, the char fraction contains inorganic materials ashed to varying degrees, any unconverted organic solid and carbonaceous residues produced from thermal decomposition of the organic components. The liquid fraction is a complex mixture of water and oxygenated aliphatic and aromatic compounds. For highly cellulosic biomass feedstocks, the liquid fraction usually contains acids, alcohols, aldehydes, ketones, esters, heterocyclic derivatives and phenolic compounds. The tars contain native resins, intermediate carbohydrates, phenols, aromatics, aldehydes, their condensation products and other derivatives. The pyrolysis gas mainly contains CO_2, CO, CH_4, H_2, C_2H_6, C_2H_4, minor amounts of higher gaseous organics and water vapour (Yaman, 2004).

Under slow pyrolysis regime (heating rates < 50 °C/min) primary wood degradations starts at about 230 °C, fast devolatilisation rates are attained at about 300 °C, and the process is practically terminated at 430 °C (Di Blasi and Branca, 2001). The yield of charcoal is promoted, particularly when the residence time of vapour and the system pressure are allowed to rise. Flash pyrolysis process is the best option to maximise the gas fraction: heating rates > 60 °C/min and temperatures $>$ 600 °C. The fast pyrolysis regime, associated with high heating rates and moderate temperatures (about 500 °C), leads to the highest yields of liquid products (Manyà, 2002). "Micro-particle" pyrolysis involves biomass materials with samples sizes sufficiently small that diffusion effects become negligible and the pyrolysis is kinetically controlled. This is a desirable situation for experiments focusing on identification of kinetic schemes. Critical particle size estimates for kinetic control are generally 100 a 1000 micrometers (Miller and Bellan, 1997).

Several thermal analysis techniques have been used to obtain the experimental data. Those most common and suitable for fundamental kinetic characterization are thermogravimetry (TG) and isothermal mass-change determination. In a thermogravimetric system a sample is exposed to a heating program at heating rates lower than 100 °C/min and the weight loss is simultaneously registered. The ability of these systems to work with very small samples and until moderate heating rates are the keys to reducing the impact of secondary vapor-solid interactions, and allow to work under conditions assuring kinetic control (Antal and Várhegyi, 1995). However, TG is limited for high heating applications, where thermogravimetric results are not reliably extrapolated. Isothermal mass-change determination has been mostly applied to analysis of the products evolution separately accounted, as function of the operation conditions. These systems admit high heating rates and large mass samples, but these are precisely the conditions which aggravate heat transfer limitations, and question the validity of the kinetic parameters obtained directly from the experimental results.

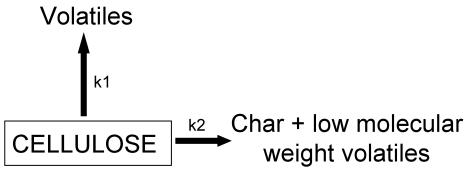

Figure 2.1: Scheme proposed by Broido and Nelson (1975) for cellulose pyrolisis.

2.2 Pyrolysis kinetics. Current state of knowledge

2.2.1 Primary decomposition

Given the key role played by the devolatilization stage in the conversion processes, numerous researchers have intensively investigated the kinetics of cellulose and biomass pyrolysis for nearly half a century (See, for example the review of Antal and Várhegyi (1995)). As far as empirical modeling concerns, the main proposed kinetic mechanisms are based either on a one step reaction (global decomposition) or on several competitive parallel reactions. All of them constitute derivations of a summative model for pyrolysis, firstly proposed by Shafizadeh and McGinnis (1971) and still widely accepted today.

The competitive outlines refer to parallel, irreversible and first order reactions to get the different fractions of pyrolysis products. One of the first approach in this field, was published by Broido and Nelson (1975), who used the results of primary thermal decomposition of cellulose to rationalize the competitive reaction model displayed in Figure 2.1. In order to take into account the reactivity of the condensible fraction, and the corresponding formation of char and gas by secondary reactions, Shafizadeh and Chin (1977) proposed a parallel reactions mechanism for the primary and secondary decomposition that allows to predict the evolution of each main product fraction (see figure 2.2). This typology of models is known as "Broido-Shafizadeh models", and are based on a distributive approach of the process. In the majority of the cases, these mechanisms have not been validated by thermogravimetry or under conditions assuring kinetic control.

The mechanisms of global decomposition describe the thermal degradation by means of an irreversible and single step reaction (Antal and Várhegyi, 1995) (see equation 4.2) to predict the overall rate of volatiles release (i.e., mass loss), but without separately predict the production of condensible and gas from volatile product. The corresponding experimental studies have been mostly carried out with small particles, employing thermogravimetric systems.

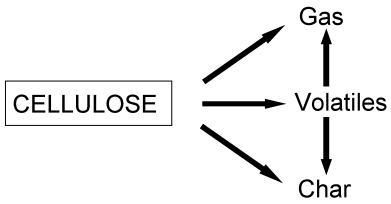

Figure 2.2: Pyrolitic mechanism proposed by Shafizadeh and Chin (1977).

$$d\alpha/dt = Aexp(-E/RT)(1-\alpha)^n \tag{2.1}$$

Here α is the conversion (reacted fraction), A is the preexponential factor, E is the apparent activation energy, R the gas constant, and n is the reaction order.

Most of the work done in this field has been reviewed by Antal and Várhegyi (1995). From diverse thermogravimetric studies they established that the primary pyrolysis of a small, homogeneous sample of pure cellulose (free of inorganic contaminants, with a well defined degree of polymerization and crystallinity), at low to moderate heating rates, was an endothermic process, modeled reasonably well by a simple first-order reaction with activation energy of 238 kJ/mol, under conditions which minimize vapor-solid interactions and heat transfer intrusions. Although the corresponding values of the activation energy published by several authors widely varied, Antal et al. explained this fact by the different sample characteristics employed (size and wood variety), the mathematical treatment of the experimental data, or in the specific case of lower activation energies (130-140 kJ/mol) observed under high heating rates, it resulted from severe heat transfer limitations. To specify the serious trouble that supposes those experimental errors, Grønli et al. (1999) coordinated the realization of a round-robin kinetic study for the cellulose pyrolysis (Avicel PH-105) in eight European laboratories. Results confirmed the theories of Antal and co-workers and evidenced the potential role of varied systematic errors in temperature measurement among the various thermobalances used by researchers.

As well as for cellulose, wide interest in the primary pyrolysis of whole biomass has appeared in the literature. The main pyrolysis reactions have already been identified (Shafizadeh, 1982; Evans and Milne, 1987; Faix et al., 1988; Várhegyi et al., 1989a). Faix et al. (1988) and Várhegyi et al. (1989a) showed that thermogravimetric analysis of small samples of lignocellulosic materials at low to moderate heating rates usually evidences a distinct DTG (differential weight loss curve) peak resulting from the decomposition of cellulose, a lower temperature process associated to hemicellulose pyrolysis, and an attenuated shoulder that can be attributed to lignin

decomposition. This is because lignin decomposes slowly over a very broad range of temperatures, providing a gently sloping baseline to the DTG curve (Evans and Milne, 1987). Sometimes the first peaks merge into one very broad peak. In an early paper Várhegyi et al. (1989b) showed that the mineral matter present in the biomass samples can highly increase the overlap of the partial peaks in DTG curves. Later several other studies evidenced the ability of pretreatments to separate merged peaks, displace reaction zones toward higher temperatures, decrease char yield and increase peak reaction rates (Várhegyi et al., 2004, 1994; Di Blasi et al., 2001a,b; Manyà et al., 2003). Of these pretreatments, the water washing is preferred because it results in less hydrolysis and solubilization of the holocellulose. Also the acid washes appeared to decrease the measured activation energy of cellulose pyrolysis (Antal and Várhegyi, 1995; Mészáros et al., 2004a).

Thermogravimetry has proved to be a useful tool in elucidating the decomposition of various biomass materials. The temperature domains of moisture evolution and hemicellulose, cellulose and lignin decomposition more or less overlap each others. The merged DTG peaks of whole biomass did not lend themselves to meaningful kinetic analysis, but the pretreatments evidenced a summative analysis of the process. Since that, numerous authors have considered that general biomass pyrolysis behaves as a superposition of the independent kinetics of the primary components (hemicellulose, cellulose, and lignin). Consequently, the global production of volatile matter corresponds to the summation of the individual contributions from these natural polymers (addition principle). Alves and Figueiredo (1988), Koufopanos et al. (1989), Font et al. (1991), Varhegyi et al. (1994) and Grønli et al. (2002) used this approach with different biomass samples and showed good reproducibility of the measurements.

Usually the mass loss or mass loss rate is described by models assuming biomass as the sum of pseudocomponents, or fractions of the biomass components decomposing in similar way and in similar temperature ranges. This idea was firstly introduce by Orfao et al. (1999), who defined three pseudocomponents for describing the primary thermal decomposition of pine and eucalyptus woods. Later Manyà et al. (2003) and Mészáros et al. (2004b) showed satisfactory results when several partial reactions for corresponding pseudocomponents were assumed in the decomposition of a wide variety of biomass materials.

In the attempt to better identify the zones associated with the devolatilization of the biomass components and their overlapped kinetics, different $T(t)$ heating programs have been employed. Mészáros et al. (2004b) increased the information content of the experiments by involving successive isothermal steps (stepwise heating programs) into their study. This approach required more partial peaks than the studies based only on linear $T(t)$ programs (Teng and Wei, 1998; Várhegyi et al., 1989a, 1994, 1997; Teng et al., 1997; Manyà et al., 2003).

Mechanisms of pyrolysis of the hemicelluloses and lignins, which are chemically different from species to species, have been less well understood, being the result of a set of complex reactions. In the attempt to elucidate these chemical complexities, various researchers (Jakab et al., 1997, 1995; Orfao et al., 1999; Manyà, 2002) have investigated the chemical behaviour of several biomass model compounds independently (e.g. xylan, isolated hemicellulose, mildly isolated lignins and technical lignins pre-

pared by steam explosion). Varhegyi and coworkers observed two characteristic peaks on the thermal decomposition of 4-Methyl-D-glucurono-D-xylan, under heating rates between 2 and 80 °C/min, and approached their kinetics by the assumption of successive reactionsVárhegyi et al. (1989a, 1997). From studies on lignin decomposition it has been established that the pyrolysis of this compound cannot be satisfactorily well described by simple kinetics (Orfao et al., 1999; Manyà, 2002). In this sense some authors have applied different order reactions to describe formally the various inhomogeneities of the main biomass components (Manyà, 2002; Manyà et al., 2003; Mészáros et al., 2004b).

In the recent years a consensus appears to emerge on the identification of the primary decomposition processes and to the appropriate requirements for the kinetic control in the thermoanalytical experiments. Current works aim at establishing simple unified mechanisms that describe the behavior of the samples in a wide range of experimental conditions, taking into account the systematic experimental errors. Antal et al. (1998) proved that the volatilization process of several cellulose samples under different heating rates could be well represented by a simple, single-step, irreversible, first-order rate law with a single value of activation energy, whereas different values of log A accounted for variations in systematic thermal lag at high heating rates and for the inherent differences in the cellulose samples. Grønli et al. (2002), Várhegyi et al. (2004) and Mészáros et al. (2004b) showed that different biomass samples or a given sample with different pretreatments can be described by similar kinetic parameters.

As an alternative instead of summative models based on first order equations, Orfao and coworkers mentioned the use of a model based on a continuous distribution function of energy activations (Orfao et al., 1999). That kind of models is mainly based on the Anthony and Howard's model (Anthony and B.Howard, 1976), for which is assumed an infinite number of parallel equations with different values of energy activation but with the same preexponential factor, coupled with a Gaussian function. Using that model for all of the three main biomass components and assuming the addition principle, Biagini et al. (2002) got to reproduce experimental results of pyrolysis of pine satisfactorily, but the corresponding fit with the simulated curves was not better than that obtained using more simple additives models.

Experimental measurements of the pyrolytic behavior of biomass at high heating rates have been the focus of extraordinary interest in the research community, but practical problems associated with these measurements have often been overlooked. The most important errors are connected to problems of temperature measurements and to the self cooling/self heating of samples due to heat demand by the chemical reaction. A consequence of these limitations is that the single step activation energy measured at high heating rates is almost always lower than its true value. Another consequence is that weight loss is reported at temperatures much higher than it actually occurs (Antal and Várhegyi, 1995). If heat transfer effects cannot be neglected, then the kinetic model may not be adequate for describing the behavior of the process involved, and must be combined with heat transfer equations. However, heat transfer problems in a real thermoanalytical apparatus are very complex. It is difficult to combine a realistic modeling of the heat transfer phenomena with complex chemical kinetic models. An alternative way is the empirical assessment of systematic errors.

In their revision of the cellulose pyrolysis kinetics, Antal and Várhegyi attributed the declining values of E and $\log A$, obtained from the independent kinetic analysis of Avicel cellulose at heating rates between 1 and 65 °C/min, to thermal lag problems with their instrument and not a shift in reaction pathways (Antal et al., 1998). Consequently they suggested the approach of a single value of E together with an uncertainty in the $\log A$ term accounting for the temperature measurement errors. Mészáros et al. (2004b) recommended an approximate modeling of the systematic errors, as additional parameters within the kinetic model.

2.2.2 Secondary decomposition

The least understood aspect of pyrolysis is the interaction of the nascent, hot pyrolysis vapors with the decomposing solid, which vapors must traverse during their escape to the environment. That process has been identified by many authors as secondary decomposition. The interaction involves an exothermic reaction which leads to the formation of char. The role of such reactions is minimized by conditions which facilitate rapid mass transfer (Antal and Grønli, 2003). The majority of studies dealing with secondary reactions have been based on sensitivity analysis but a few number of practical models have included it.

The TG experiments conducted by Várhegyi et al. (1988a) and the series of differential scanning calorimetric (DSC) experiments reported by Boer and Dufie (1985) and Mok et al. (1992) showed that high char yields are derived from high concentrations of vapor phase pyrolysis products held captive in closed crucibles. The DSC studies showed small samples of wood undergoing endothermic pyrolysis, whereas samples with larger particle sizes exhibited exothermic pyrolysis. Mok and his coworkers observed a linear relationship between reaction exothermicity and char yield. They found that a decrease in the velocity of purge gas passing through the sample increased the charcoal yield from 6% to over 21% at 0.1 MPa. An increase in pressure from 0.1 to 1.0 MPa (with a constant purge gas velocity) further increased the charcoal yield to 41%.

Concerning kinetic modeling, Di Blasi and Russo (1994) presented an approach describing the kinetics according to a competitive reaction scheme. Secondary decomposition was included as tar cracking to light hydrocarbons, though tar polymerization to char was ignored. Babu and Chaurasia (2003) presented a mathematical model to describe the pyrolysis of a single solid particle of biomass coupling the heat transfer equation with the chemical kinetics equations. The majority of the generalized models correspond to extremely complicated schemes and suffer from a high number of undefined parameters, lack in the interrelation with the biomass composition, or they have not been validated for a sufficiently wide range of experiment conditions.

2.2.3 Heat of reaction

The involved heat of reaction has an important influence on the course of thermal conversion. Although a substantial amount of information about thermal properties of some biomass, like wood, can be traced in the literature, few values have been

reported for the heat of reaction of specific lignocellulosic materials. The literature on biomass pyrolysis report varied and contradictory results for heat of reaction, ranging from endothermic to largely exothermic values. Unavoidable secondary reactions between volatiles and char, as well as autocatalytic effects due to impurities, are usually assumed to be the reasons for these differences (Antal and Grønli, 2003; Rath et al., 2003).

Under slow pyrolysis, small particles of cellulose and some woods underwent global endothermic behaviour, whereas samples with larger particle sizes exhibited exothermic pyrolysis (Antal and Várhegyi, 1995). This is explained by the enhanced interaction of the hot pyrolysis vapors with the decomposing solid, that involves an exothermic reaction which leads to the formation of char. The effect of the highly endothermic nature of the cellulose pyrolysis on the unavoidable thermal lags in temperature measurements was thoroughly discussed by Antal et al. (1998) in their revision of the cellulose pyrolysis kinetics.

Differential scanning calorimetry (DSC) has been proved to be an effective technique for the obtainment of reliable values of the elementary heat of reaction in the absence of complicating phenomena, as heat or mass transfer limitations. Stenseng et al. (2001) and Rath et al. (2003) investigated the influence of sample size on the pyrolysis of different kind of biomass by simultaneous thermogravimetric analysis coupled to a DSC calorimeter. Rath reported a linear correlation between the heat of the primary pyrolysis process and the final char yield. This strong dependency, that is in turn highly sensitive to the experimental conditions, can explain the uncertainty of the data for the heat of wood pyrolysis reported in the literature.

2.2.4 Products distribution

A number of reviewers of biomass pyrolysis have postulated more or less complex reaction schemes to account for slow and fast pyrolysis and primary and secondary gas phase pathways. These range from simple scheme to complex, multipath scheme (Shin et al., 2001). One of the most important findings in the reaction pathways topic was presented by Piskorz et al. (1988), related to a major pyrolysis pathway which leads to the selective formation of glycolaldehyde from cellulose. As a result of those findings, two major pathways are now recognized to be active during cellulose pyrolysis: one which leads to the formation of levoglucosan as a relatively stable product and the second which yields glycolaldehyde (Antal and Várhegyi, 1995). In a series of important papers it was established the influence of salts and metal ions on the productivity of the two pathways (Antal and Várhegyi, 1995; Evans and Milne, 1987). Those substances can drastically change the product slate, inhibiting the formation of levoglucosan and leading to a different product state and an increase in char yield. Less information has been presented for hemicellulose, for which has been associated a similar distribution of pyrolysis products as cellulose. In the case of lignin, it is well known that its thermal decomposition occurs in a broad temperatures range resulting in a 30 - 50% char and a significant amount of low molecular mass volatiles, in addition to the monomeric and oligomeric products (Evans and Milne, 1987). In summary, primary pyrolysis vapours are rather low in molecular weight,

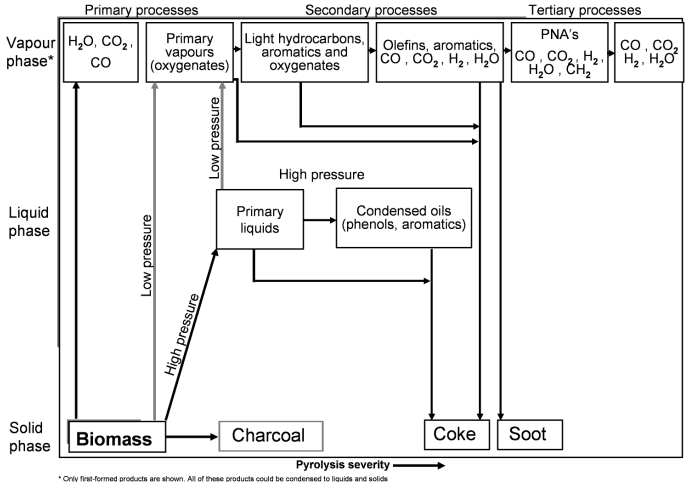

Figure 2.3: Pyrolysis reaction pathways summarised by Evans and Milne (1987).

representing monomers and fragments of monomers of the biopolymers of biomass.

Most of the studies concerning reaction pathways in biomass pyrolysis are limited to a qualitative point of view. Evans and Milne summarized their observations on the pyrolysis pathways for whole biomass and its components as the diagram shown in figure 2.3. Few works are found in the literature that model biomass pyrolysis predicting yields and evolution patterns of selected volatile products as a function of feed stocks characteristics and process conditions. Several analytical methods, such as TG/MS (Thermogravimetry/Mass Spectrometry), MBMS (Molecular Beam Mass Spectrometry), Py/GC (Pyrolysis/Gas Chromatography), GC/MS, HPLC (High Performance Liquid Chromatography) and FTIR (Fourier Transformer Mass Spectrometry) have been applied to determine individual product yields. Wójtowicz et al. (2003) coupled low heating rate data obtained from a thermogravimetric analyzer to a FTIR device to perform kinetic analysis of tobacco pyrolysis. The results were used to create input to a biomass pyrolysis model based on first-order kinetic expressions with a Gaussian distribution of activation energies for each volatile species. Given the tremendous diversity of biomass products, extreme detail in the prediction of each individual evolved species has led to impractical and complicated models with high number of unknown parameters. Those approaches carry a level of ill-definition in the model on the one hand, and a over-simplification of the chemistry process when first order reactions are assumed. First order test is used when is known to undergo unimolecular decomposition. However, in biomass pyrolysis there is the possibility for other type of reaction mechanisms due to the high chemical complexity.

2.2.5 Data analysis

Kinetic analysis

The data handling and the criteria used to determine the 'best' kinetics parameters that reproduce the experimental results is a crucial target of the kinetic modeling. In the early days of thermal analysis the kinetic evaluation was based on linearization techniques, plotting various functions of the experimental data against 1/T. These methods have usually uneven sensitivity on the uncertainty of the experimental data (due to the logarithms involved) and/or do not exploit fully the information content of the experiments. The real complexity of the processes has required more accurate models, thereby increasing the number of the unknown parameters. The determination of the higher number of unknown parameters has leaded to the simultaneous evaluation of whole series of experiments. The non-linear methods of least squares, which are generally employed in other areas of science, have showed to be useful (Várhegyi et al., 2001).

The use of the non-linear method of least squares in non-isothermal kinetics dates back to the pioneering work of Broido and Weinstein (Broido and Weinstein, 1971), and has been spreading gradually since then. The most common criterion for the objective function used to evaluate the quality of the model is to minimize the differences between the calculated and experimental values of the weight fraction (integral form) or the time derivatives of weight (differential form). Weight fraction curves are not very sensitive to processes that can superpose partially or even go unnoticed. The differential objective function is much more sensitive to these changes but care must be taken in the calculation of the derivative because small experimental errors or deviations can produce large errors with respect to the actual derivative curve (Várhegyi et al., 2001).

Product distribution analysis

Given the large data sets collected in thermoanalytical studies, e.g. mass spectrometric analysis or FTIR measurements, several authors have introduced multivariate statistical methods (Principal Components Analysis), to help in the interpretation of the trends on the experimental results (Winding and Kistamaker, 1981; Evans and Milne, 1987; Mészáros et al., 2004a; Statheropoulos and Mikedi, 2001; Pappa et al., 2003). Those techniques provide a mean of simplifying pyrolysis data by finding correlations between variables. This data reduction makes possible graphical display of the data that not only show trends but also can provide chemical insight into the transformations.

2.3 Pyrolysis kinetics: trends and challenges

The following list enumerates the main troubles found on analyzing the current approaches for pyrolysis kinetics:

- Widely different kinetic parameters have been published in the literature on biomass pyrolysis. This is the outcome of an attempt to force the rate law to mimic weight loss that occurs at each set of different experimental conditions, with various experimental problems, and the occasional use of unsuitable evaluation methods. The consensus on the identification of the primary decomposition processes still needs major efforts on representing quantitatively the observed similarities between the different sort of samples analyzed on the one hand, and predicting phenomena in a very wide range of experimental conditions on the other hand.

- Much of the disagreement in the literature concerning to the data obtained by TGA work has been due to the influence of varied systematic error associated with the characteristics of the originating equipment and the experimental procedure. As Gronli and coworkers established a reference on kinetic data from Avicel cellulose to ensure the reliability of untrustworthy TGA data (Grønli et al., 1999), an agreement is still required on the definition of the experimental procedures to get reliable kinetic data from whole biomass.

- While most work has been carried out on wood, a few studies on detailed thermogravimetric-reaction kinetic analysis of energy crops have been reported. Besides, the woody materials traditionally employed in the pyrolytic studies correspond to very homogeneous samples, for laboratory tests, that hardly approach a real heterogeneous residue. The quantity of woody residues remaining largely unused, in addition to the increased exploitation of herbaceous crops, urgently ask for a better description of both the dynamics and the influence of the heterogeneities on biomass thermolysis.

- At the time being the understanding of the effects of pretreatments remains largely qualitative. The various industrial applications (e.g. the production of charcoal, activated carbon and liquid fuels) require a clear understanding of the variations in the original composition and the effects of the pretreatments, since the yields and the composition, structure, and other properties of the products are highly influenced by the properties of the feedstock.

- The traditional employment of linear heating programs in thermogravimetric experiments has not guaranteed an in-depth characterization of the various pyrolytic processes occurring in the material. The chemical heterogeneities of the biomass components and the physical heterogeneity of the plant materials increase the overlap between the independent kinetics. Consequently, superposed reactions could be unnoticed if the evaluation is based only on linear heating programs. Continued effort on increasing the information content of the experiments, by coupling some other heating approaches or/and analysis of the evolved products, is still necessary.

- Empirical models are criticized due to over-simplification of extremely complex chemical and physical phenomena on the one hand and focus only on total devolatilization (without counting product fractions separately) on the other hand.

These kinds of models are not enough for scale-up attempts. Increasingly interest exists for comprehensive biomass pyrolysis models that could predict yields and evolution patterns of selected volatile products as a function of feedstock characteristics and process conditions. These classes of studies can be useful for the selection of the most appropriate configuration and operating conditions of chemical reactors on dependence of the desired composition and yields of the products.

- Mathematical models of biomass pyrolysis coupling chemical processes (including secondary reactions) and transport phenomena are rarely available in the literature. There is still a lack on fundamental research to improve design methods and modeling involving primary and secondary reactions, leading to optimal reactor design and process. Being pyrolysis the initial step in all the thermal conversions of biomass materials, including combustion and gasification, a coupling of pyrolysis kinetics to the corresponding models of those thermal processes would be a real boon.

2.4 Thesis objectives

In the sections before, the current approaches for biomass pyrolysis kinetics have been carefully analyzed and their limitations highlighted. In general, this thesis will deal with the existing shortcomings in the aforementioned approaches, on the bases of fundamental research.

The principal contribution of this thesis will lie in building up a reliable and integrated thermokinetic approach for biomass pyrolysis that is able to predict phenomena in a wide range of experimental conditions and for different type of biomass material. This approach will be progressively constituted by the analysis of several results coming from different thermoanalytical techniques: thermogravimetry, differential scanning calorimetry, TG/MS and and TG/FTIR. These techniques allow to study the entire pyrolytic process, including primary and secondary decomposition, as well as the analysis of characteristic products evolved.

Besides, the present thesis aims for the clarification of the thermal properties of important feed stocks that have not attracted yet sufficient attention in the biomass studies. The woody residues of the carpentry industry remain largely unused and present a solid waste disposal problem. Herbaceous crops produced in energy plantations are already raw material of power generation plants, although much remains to be learned about its thermochemical properties.

The final intention with this thesis is to contribute to a consensus on the description of the decomposition processes, as well as on the integration of the different phenomena making up biomass pyrolysis. The idea is to help in the understanding of the process as a whole, in such a way that the corresponding kinetics can be integrated into the modeling of reactors for thermochemical upgrading.

Some of the most relevant aspects to be considered are:

- In-depth analysis of the extension of systematic errors in the thermogravimetric

studies performed in this thesis.

- Analysis of several evaluation strategies to obtain the best-fit kinetic parameters for the description of the global decomposition, for different heating programs and biomass compositions.
- Qualitative and quantitative analysis of the evolution of characteristic pyrolysis products in vapor and gas phases.
- Qualitative and quantitative study of the intrusion of secondary reactions during the process, from the analysis of the samples thermal behavior.

Chapter

THREE

Thermogravimetric study

This chapter exposes the experimental procedure followed in the thermogravimetric studies carried out along this work, as well as general features on the thermal behavior of the samples. The experimental system is defined by the type of biomass materials and pretreatments, as well as the different thermogravimetric apparatus and experimental procedures employed in this thesis. The extent of systematic errors associated to the experimental part is deeply observed. Given the large data sets collected in this thesis, we have used a chemometric evaluation tool (PCA) for a preliminary characterization of the thermogravimetric results.

3.1 Introduction to the thermogravimetry

In the chapter before, some concepts related to thermogravimetry were introduced. This technique allows a simultaneous register of both weight loss and thermal history of a sample exposed to a heating program. The ability of these systems to work with very small samples and until moderate heating rates are the keys to work under conditions assuring kinetic control.

In general, for conventional thermobalances the maxim value of heating rate is limited around 100 °C/min. The use of severe heating programs entails large thermal gradients (i.e., the differences between the true sample temperature and the furnace thermocouple temperature) because of heat transfer limitations intrusions. Thus, low heating rates (generally up to 40 °C/min) are preferred in kinetic studies. On the other hand, particles larger than 1000μm can suffer by relatively large diffusion effects which can strongly affect the pyrolysis evolution due to internal and external temperature gradients, heat capacity effects, and also temperature variations resulting from endothermic (or exothermic) reactions.

Normally, biomass particles are distributed in cylindrical shaped holders or crucibles. Inert gases (i.e., helium, argon or nitrogen) are used in order to remove vapor pyrolysis products. He has a higher thermal conductivity than N_2 and, consequently, minimizes the temperature difference between sample and gas. However, nitrogen is

more commonly used as purge gas in thermogravimetric studies, without entailing important heat transfer problems due to the type of gas itself. Argon is more suitable in the case of studies measuring gaseous species, e.g. mass spectrometry. The Argon isotope at m/z 38 is used as an inner sensitivity calibration signal.

Many authors have emphasized the importance of calibration in thermogravimetric analysis (See, for example the review of Antal et al. (1998)). Measurements of the nickel Curie-point transition, as well as the melting point of different metal standards are the procedures most commonly used for periodic calibration of the thermogravimetric instruments.

The history of the field teaches that all TGA data is untrustworthy unless some effort is made to calibrate the TGA or otherwise verify its reliability. As it was pointed out in the chapter before, Grønli et al. (1999) organized a round robin study that established a reliable range of weight loss data and kinetic values for Avicel cellulose pyrolysis. An easy way to prove that TGA data is reliable is then comparing an Avicel cellulose pyrolysis curve with the round-robin data of Gronli and coworkers.

3.2 Experimental system

3.2.1 Biomass materials

In the description of the thesis scope (Section 2.4) we emphasized our intention to examine materials that have not been extensively considered in previous studies, even though they represent a waste disposal problem and/or have substantial energy and chemical potential. Basically, we have chosen three biomasses: two woody residues of the carpentry industry and an energy crop. Other material, which will be used for the application of the kinetic schemes, will be described in a further chapter.

The woody materials correspond to pine and beech chips taken from Barcelona's carpentry residues. Since the samples were collected in situ, they are mixtures of unspecified Mediterranean species. We are unaware of previous studies on a detailed thermogravimetric-reaction kinetic analysis of these type of residues, instead of the numerous publications concerning pyrolysis of homogeneous wood for laboratory tests.

The herbaceous sample corresponds to artichoke thistle (cynara cardunculus), which came from a specialized crop, developed for investigation in the Spanish province of Soria. The sample is a mixture of buds, branches, fibers and stalk fragments from mature shoots. This species attracts great local attention due to the suitable climate and soil conditions, in addition to recognized potential for energetic purposes, for paper pulp or animal feeding. The current research activity is mainly focused on the optimal plantation conditions (e.g., cultivation, growth, cutting and harvest) for energy production and commercialization[1]. Thistle is already used as a raw material for an electric power generation plant in Spain, although much remains to be learned about its thermochemical properties[2].

[1] Ciemat. Producción y evaluación de recursos de biomasa, 2 February 2006, <*http://www.ciemat.es*>.

[2] Las primeras plantas de biomasa a partir de cultivos energéticos en España, 2 February 2006, <*http://www.infoenergia.com*>.

Figure 3.1: Cynara cardunculus.

3.2.2 Sample pretreatments

The increased exploitation of biomass materials different from those usually investigated requires a better description of both the dynamics and the influence of the heterogeneities on biomass thermolysis. Several factors may influence the thermal behavior of plant materials. The inorganic ions are known to exert a great influence on the thermal degradation of the natural polymers that make up biomass (See the literature review, Section 2.2.1). The extractive content of the samples is also known to affect the kinetic behavior (DeGroot et al., 1988; Di Blasi et al., 2001a; Várhegyi et al., 2004) although there is still a lack of conclusive evidence of the intrinsic effects on the pyrolysis process. The understanding of the variations in the original composition is a key factor in industrial applications, too, since the yields and the composition, structure, and other properties of the products are highly influenced by the properties of the feedstock. The yield of charcoal is favored by the presence of some mineral elements in the biomass ash (Antal and Grønli, 2003). However, the content of salts and minerals can cause corrosion, fouling and slagging in biomass plants (Stenseng et al., 2001; Várhegyi et al., 2004). Some studies have reported higher yields of charcoal from extractive-rich woods (Di Blasi et al., 2001b). The effect of the extractives on phase separation of pyrolysis liquid fuels has been also studied (Oasmaa et al., 2003a,b).

To study the influences of feedstock properties, special attention has been given to the effects of pretreating the materials on the kinetics. In the present work, for the investigation of the role of inorganic ions, a part of these ions was removed by water-washing (a hot water bath at 80 °C during 2 h), according to the procedure suggested by several authors (Antal and Várhegyi, 1995; Teng and Wei, 1998). For the study of the effect of the extractives, samples were extracted with ethyl alcohol, for about 24 h in a Soxhlet apparatus, following a standard methodology for the determination of extractives in biomass (Brown et al., 2003). Thus, the range of evaluated samples involves untreated, water-washed and ethanol-extracted samples, as well as samples subjected to both water-washing and ethanol extraction.

3.2.3 Chemical composition of the samples

The proximate analysis, elemental composition, and extractive content of the samples are shown in Table 3.1. Information concerning chemical composition of Mediterranean biomass materials is presented in Table 3.2 as a reference.

Table 3.1: Biomass samples analysis [A.1.4]

	Proximate (% by weight)			
biomass	moisture	volatile matter	fixed carbon	ash
untreated pine	7.53	71.63	19.84	1.00
washed pine	3.29	77.98	18.14	0.60
untreated beech	7.03	73.62	19.11	0.24
washed beech	2.35	79.05	18.41	0.20
untreated thistle	11.1	63.39	17.41	8.10
washed thistle	2.43	70.79	22.01	4.77
	Ultimate (% by weight; dry ash-free samples)			
biomass	C	H	N	O
untreated pine	46.56	6.48	< 0.10	46.96
washed pine	43.37	6.68	< 0.10	49.95
untreated beech	45.68	6.52	< 0.10	47.80
washed beech	47.43	6.55	< 0.10	46.02
untreated thistle	40.45	6.07	1.08	52.40
washed thistle	45.04	6.7	0.97	47.29
Extractives (% by weight; untreated samples)				
pine		beech	thistle	
4.85		1.15	6.1	

3.2.4 Thermogravimetric apparatus and experimental procedures

The present study included five widely used thermobalances from three different laboratories. Table 3.3 summarizes the manufacturers' technical specifications of these instruments. Some of these apparatus worked on-line with other thermoanalytical techniques. Both Setaram and Netzsch thermobalances are simultaneous thermogravimetry/differential scanning calorimetry (TG/DSC) analyzers, used for the analysis of heat flows in Chapter 6. Metallic crucibles, with greater thermal conductivity, were preferred in these cases. A set of the experiments with the Netzsch thermobalance were performed coupling an FTIR spectrometer for the on-line analysis of volatile products under different conditions (Chapter 6). The experiments in the Perkin-Elmer equipment were TG/MS measurements (Chapter 5), using high-purity argon as purge gas instead of nitrogen.

Table 3.2: Chemical analysis of biomass samples on a dry basis

	holocellulose	**lignin**	**extractives**	
species (botanical name)	wt %	wt %	wt %	ref
beech (Fagus sylvatica)	78	20	2	Grønli et al. (2002)
pine (Pinus pinea)	69	24	7	Grønli et al. (2002)
thistle (Cynara cardunculus)	65	30	5	Antunes et al. (2000)

Table 3.3: Characteristics of the thermogravimetric instruments

	Cahn TG-151	**Setaram Setsys 12**	**Perkin-Elmer TGS2**	**Netzsch STA 409/C**	**TA Instruments**
Source	UPC laboratory	UPC laboratory	Hungarian Academy of Sciences	Universita degli Studi di Pisa	Universita degli Studi di Pisa
Balance sensitivity (μg)	10	0.03	0.1	1	0.1
Sample capacity (mg)	100	200	130	2000	200
Thermocouple location	Below a sample holder	Below and in contact with a crucible holder	Below a sample holder	Below and in contact with a crucible holder	Above a sample holder
Calibration	Decomposition of calcium oxalate monohydrate	Melting point of different metal standards	Curie point of different metal standards	Melting point of different metal standards	Curie point of different metal standards

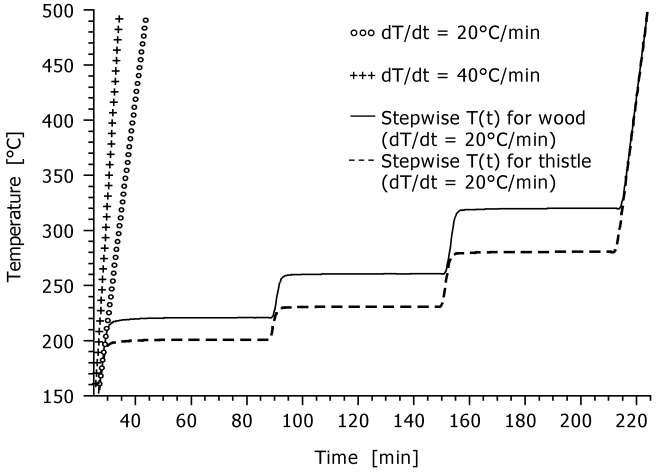

Figure 3.2: Heating programs for the kinetic studies. [A.1.3]

All the experiments were performed under atmospheric pressure. Particles of sizes below 1 mm were distributed evenly. The heating programs, gas flows and selected initial sample masses will be described in a further section. Buoyancy corrections were performed according to the standard procedures employed in each laboratory. Experiments from the Cahn thermobalance as well as both TG/DSC analyzers required correction of buoyancy effect by subtracting the TG signal of empty sample runs.

3.2.5 Temperature programs

Two types of heating programs (linear and stepwise) were used in this work (Figure 3.2). The stepwise temperature programs were included to obtain enough information for the reliable determination of the unknown parameters. The corresponding steps were selected for each interesting region in the pyrolysis process: at the low temperature phenomena, at the start of the main hemicellulose decomposition and at the start of the main cellulose decomposition. The same temperature program was employed for both woods. In the case of thistle lower temperature steps were used since the devolatilization takes place at lower T values. The stepwise experiments took place in longer time intervals than the ones at linear temperature programs. Their DTG peak maxima were 10 - 70% of the values of the corresponding linear $T(t)$ experiments at 20 °C/min. Accordingly the peak values of the heat flux required by the endothermic reaction were also much lower in the stepwise experiments. An additional linear heating program, 40 °C/min was introduced to clarify better the unusual behavior of the herbaceous biomass. In this chapter, we focus on the linear heating rate programs. The stepwise experiments will be considered in the next chapter.

3.2.6 Design of experiments

The pyrolytic behavior of a biomass samples is reflected by the specific weight loss and thermal history, the heat flow answer and the evolution of the different product species, among other instances. We have learned that some of the main variables affecting the process are substrate composition, heating conditions (heating rate, temperature programs), pressure and flow of the surrounding gaseous environment, size of particle, layer thickness (not the mass itself) and possibility of autocatalysis by volatile pyrolysis products. From the available sources, we chose some of these variables to analyze our system of work. Designing the set of experiments, we considered the following assumptions so as to assess the sensitivity with far fewer and more practical runs than the number provided by a common full factorial approach.

- As the actual mass flux is roughly proportional to the heating rate, equivalent kinetic results can be expected, for example, from 4 mg initial sample mass at 10°C/min, 2 mg at 20°C/min or 1 mg at 40°C/min, for the same gas conditions around the samples in inert atmosphere. For primary pyrolysis, we have limited the analysis of these two variables fixing one value of initial sample mass and two values of heating rate.

- Concerning the influence of the layer thickness, 4 mg of a sample spread on a pan of Ø 4.3 mm is equivalent to 6 mg of the same sample spread on a pan of Ø 5.3 mm or 9 mg spread on a pan of Ø 6.7 mm. Since we wanted to obtain reproducible experiments from different apparatus, we tried to keep roughly equal values of layer thickness for the available crucibles. We also limited this study to the analysis of the fraction of particles below 1 mm.

- For studies using low sample masses, under atmospheric pressure, there is no conclusive evidence on the importance of the gas flow rate, as long as the product gases are swept out from its vicinity. Várhegyi and coworkers did not observe any important changes on kinetics employing 60, 80 and 140 ml/min gas flow[3]. Consequently, we did not consider the variation of gas flows in experiments obtained from the same apparatus. Note that the gas flow rates cannot be compared directly between different instruments. The actual gas velocities around the sample depend highly on the geometry of the furnace. Both the diameter of the furnace and the way that the sample is shelter due to the sensitiveness of the instruments are key factors. As long as the furnace configuration allowed it, we fixed a nominal gas velocity of around 0.005 m/s in different instruments.

In this way, the system for the analysis of primary decomposition was reduced to 12 type of samples (three biomasses with four degrees of pretreatment as explained above), one initial sample mass, one purge gas velocity, 3 temperature programs (two linear heating rates and one stepwise) and 5 thermobalances. Repetitions of the experiments in a given apparatus were also performed. Some additional considerations were taken into account to reduce even more the system. Pine and beech biomasses

[3]Várhegyi, G., personal communication.

present similarities in chemical composition. Thus, in some cases only one of them was considered or sets of their pretreated versions were selected. Since the herbaceous crop is the most heterogeneous material, more attention was focused on it. The use of several thermobalances obeyed to specific purposes. Not all the experimental conditions were reproduced in every apparatus. For a look at secondary decomposition, we also studied a small range of different initial sample masses in crucibles with and without pierced lids, limited to the Netzsch TG/DSC thermoanalyzer. This set of experiments will be deeply considered in chapter 6. Table 3.4 summaries the entire set of experimental conditions used in the thermogravimetric studies performed in this thesis.

3.3 Experimental tests with pure cellulose

In this section we present the results of kinetic studies with pure cellulose carried out in the five thermobalances. The idea is to ensure the reliability of the thermogravimetric data by comparing current results with those obtained by eight European laboratories participating in the round-robin study organized by Grønli et al. (1999). Kinetic analysis was based on the same first-order rate equation as the above-mentioned study

$$d\alpha/dt = Aexp(-E/RT)(1-\alpha) \tag{3.1}$$

where

$$\alpha = 1 - \frac{W_t - W_f}{W_0 - W_f} \tag{3.2}$$

W_t is the experimental weight at each monitoring time, W_f is the final weight, W_0 is the initial dry mass (after weight stabilization at 150 °C), A is the pre-exponential factor, E is the apparent activation energy, R is the constant gas, and T is the sample temperature. Kinetic parameters (A, E, and W_f) were estimated using a nonlinear least-squares algorithm. Results of the kinetic evaluation from all the different equipments show a satisfactory agreement with the data obtained by the other laboratories (see Table 3.5). Therefore, we consider trustworthy the data obtained in the different instruments.

3.4 Characterization of the experiments

Figure 3.3 is an example of the obtained thermogravimetric curves (TG, DTG) with the untreated samples. The pyrolytic processes, discussed extensively in the literature, are the following: the main DTG peak corresponds to cellulose decomposition (Várhegyi et al., 1989a), and the shoulder at lower temperatures (around 320 °C for wood and at about 270 °C in thistle) can mainly be attributed to hemicellulose devolatilization (Di Blasi and Lanzetta, 1997; Várhegyi et al., 1989b). Contributions from decomposition of lignin and extractives are visible as wide shoulders on the

Table 3.4: Experimental conditions used in the thermogravimetric study

		Cahn TG-151	**Setaram Setsys 12**	**Perkin-Elmer TGS2**	**Netzsch STA 409/C**	**TA Instruments**	
Samples[a]	untreated thistle	*	*	*	*	*	
	washed thistle	*	*	*	*	*	
	extracted thistle		*	*	*	*	
	washed&ext. thistle		*	*	*	*	
	untreated pine	*	*	*			
	washed pine	*	*	*			
	extracted pine		*	*			
	washed&ext. pine		*	*			
	untreated beech	*	*	*	*	*	
	washed beech	*	*	*			
	extracted beech		*	*			
	washed&ext. beech		*	*			
Purge gas		nitrogen	nitrogen	argon	nitrogen	nitrogen	
Flow rates (mL/min)		200	50	140	80	60	
Crucible material		alumina	platinum	platinum	aluminum	aluminum	alumina
Crucible diameter (mm)		6.2	4.3	6.0	5.3	5.3	6.7
Crucible height (mm)		8	4	1.4	4	4	4
Initial mass[b] (mg)		10	4	3	2 - 14[c]	6	9
Temperature programs		linear 20 °C/min	linear 20 and 40[d] °C/min, stepwise[e]	linear 20 °C/min	linear 20 °C/min	linear 20 °C/min	

[a]Sign ∗ denotes samples employed in the given equipment.
[b]Rough sample amounts.
[c]Variation in mass only for the untreated and washed samples. 6mg for the rest.
[d]Only with untreated thistle.
[e]The following samples were not subjected to a stepwise program: extracted beech, washed&ext. beech and washed&ext. pine.

Table 3.5: Kinetic studies of Avicel cellulose pyrolysis

	Kinetic parameters					Experimental conditions[a]		
	E (kJ/mol)	$\log A$ (s^{-1})	$1 - W_f/W_0$	T_{peak} (°C)	% fit [b]	cellulose Avicel	heating rate	initial weight
Gronli et al.[c]	244.0	19.0 ± 0.2	0.916 ± 0.026	327 ± 5	0.6	PH-105	5.0 ± 0.1 °C/min	4.1 ± 1.3 mg
Cahn	242.6	19.0	0.870	328	0.9	PH-101	5 °C/min	5 mg
Setaram	240.5	19.0	0.902	332	0.9	PH-105	5 °C/min	2 mg
Perkin-Elmer	236.0	18.3	0.933	328	0.4	PH-105	4.8 °C/min	2 mg
Netzsch	244.0	19.2	0.931	328	0.8	PH-102	5 °C/min	2 mg
TA	228.1	17.9	0.895	320	0.9	PH-102	5 °C/min	2 mg

[a]Same gas and purge flow as in table 3.4.
[b]Between the experimental and simulated TG curves.
[c]Mean values from the round robin study.

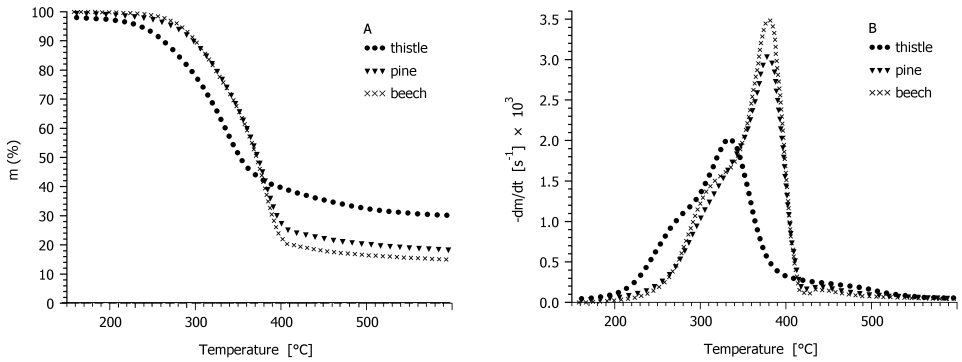

Figure 3.3: TG (A) and DTG (B) curves during pyrolysis of the untreated samples at 20 °C/min, from experiments performed in the Perkin-Elmer thermobalance.

main devolatilization domain, due to the very broad decomposition range of these components (Jakab et al., 1997; Grønli et al., 2002; DeGroot et al., 1988).

A practical way to quantitatively describe the thermogravimetric curves is by determination of several parameters related to characteristic reaction temperatures, devolatilization rates, and mass fractions. The mass loss curve and the first and second time derivatives of the mass fraction are used for such quantifications. Grønli et al. selected 10 well-defined points for the characterization of a thermogravimetric experiment of a biomass sample (Grønli et al., 2002). In this work a subset of these quantities is used, following the work of Mészáros et al. (2004b). This is shown in Figure 3.4 and listed below:

- $T_{hcstart}$ is the extrapolated onset temperature calculated from the partial peak that results from the decomposition of the hemicellulose component.
- DTG_{max} and T_{peak} are the overall maximum of the mass loss rate normalized by the initial sample mass, and the corresponding temperature, respectively.
- $T_{cellend}$ is the extrapolated offset temperature of the -dm/dt curves. This value describes the end of the cellulose decomposition.
- *Char* is the solid residue at 550 °C. This value has been selected since the main decomposition reactions have already finished at this temperature.
- $Width$ is the peak width, defined as the difference between the $T_{cellend}$ and the temperature of the shoulder of the hemicellulose decomposition. This latter temperature is the point where the second derivative of the mass fraction attains the value nearest to zero in this region.

These characteristic points will help us in the interpretation of the entire pool of thermogravimetric results. Firstly, we will observe the reproducibility from different

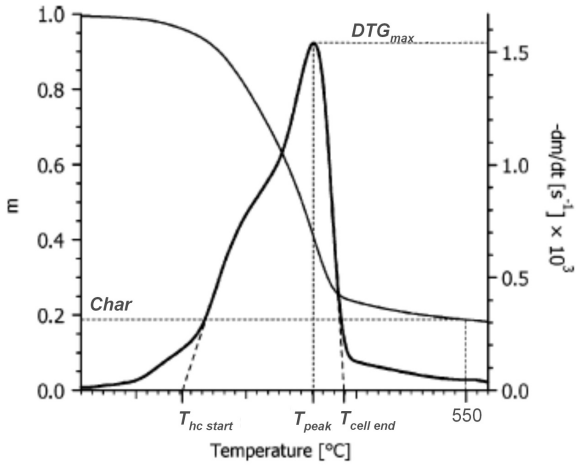

Figure 3.4: Definition of the characteristics of the thermogravimetric curves (source: Mészáros et al. (2004b)).

sources, in addition to the extent of systematic errors (which depend on the experimental conditions). Then, we will compare the thermal behavior between the different types of untreated and pretreated samples. PCA (Principal Component Analysis) is applied as the mathematical tool in these evaluations, given the large data set of thermogravimetric results collected in this thesis. Principal component analysis is a useful statistical technique which can be used to replace a large set of observed variables with a smaller set of new variables, the principal components, retaining the patterns of the original data (Jackson, 2003; Mészáros et al., 2004a; Statheropoulos and Mikedi, 2001; Pappa et al., 2003).[4] The work of Mészáros et al. (2004a) was the first one that introduced the characteristics of the DTG curve into the PCA calculations.

The repeatability of the DTG characteristics for the pyrolysis of all the samples at linear heating programs was determined in every apparatus. The maximum standard deviations of $T_{hcstart}$, $T_{cellend}$, DTG_{max}, T_{peak}, $Width$, and $Char$, were 5 °C, 4 °C, 2x10^{-4} s^{-1}, 2 °C, 4 °C, and 0.04, respectively. The mean values were introduced in the PCA calculations. We considered various data sets with the idea to differentiate the specific influence of the variables (sources, experimental conditions, types of sample and pretreatments) on the thermal decomposition.

[4]The reader should be addressed to Appendix B for a revision of the theory behind the Principal Component Analysis.

3.4.1 Influence of the originating equipment and the experimental conditions

In the attempt to observe the influence of varied systematic error associated with the characteristics of the originating equipment and the experimental procedure, we performed a PCA calculation for every type of sample, using the DTG values from the experiments under equivalent experimental conditions in different apparatus (see table 3.4). For the untreated thistle, we additionally included the mean values coming from the experiments at 40 °C/min heating rate. Results with different initial sample masses, using crucibles with and without a lid, are considered in a further evaluation. Figures 3.5 and 3.6 are examples of the PCA results, in the cases of untreated thistle and beech, respectively. The DTG values corresponding to these calculations are presented in table 3.6. The $\rho\delta$ factor (sample density multiplied by layer thickness) represents the geometry of the sample, assuming that the particles were evenly distributed in cylindrical shaped blocks. These values were not introduced in the calculations but they give us an indication of the differences in layer thickness between the observations.

The score plot (panel A in Figure 3.5 and Figure 3.6) represents the principal components' space, where the similar objects (results from different apparatus or conditions) lie close to one another, while the distance between considerably different results is large. For the herbaceous crop, the experiment at 40 °C/min (40) lies far from the rest performed at 20 °C/min. Higher heating programs are expected to affect the temperature measurements and the thermal behavior of the samples because of heat transfer problems (Antal et al., 1998; Mok et al., 1992). For the rest of the experiments, which where performed under roughly equivalent experimental conditions, some scattering is even observed on the PCA space. The Cahn result appears clearly separated from the rest at the same temperature program. Results in the Cahn equipment may be affected by several conditions. In this case, we got the highest $\rho\delta$ factor, which is associated to the layer thickness of the sample. Besides, the corresponding sample holder has the largest internal height (see table 3.4). These geometric factors, joined to the characteristics of the furnace, may compromise the flow of product gases from their vicinity, thus affecting the thermal behavior. At the same time, the Perkin-Elmer (PE) experiment, with the most different value of layer thickness ($\rho\delta$ factor), lies much closer to the rest of observations, indicating that the other conditions (geometry and configuration of the furnace) are affecting even more the Cahn results. The loading plot (panel B in Figure 3.5) represents the original variables in the field of the two first principal components. DTG_{max}, T_{peak}, $T_{hcstart}$, and $Char$ have the highest contribution on the first component. On the other hand, $T_{cellend}$ and $Width$ play the most significant role in determining the second component, in which the Cahn observation appears more distant. Scarcity in the original data highly affects the calculation of the latter DTG points, coming from the second time derivative of the mass fraction. Note that the Cahn thermobalance has the lowest sensitivity in the group of used instruments. Moreover, the corresponding data were collected every 60 s, which is far more sparse than in the rest of equipments.

The similarities in a group of results can also be represented by a hierarchical tree

Table 3.6: Characteristics of the thermogravimetric curves of untreated thistle and beech

Sample and originating equipment (Abbreviation)		$T_{hc\,start}$ **(°C)**	$T_{cell\,end}$ **(°C)**	DTG_{max} **(%/s)**	T_{peak} **(°C)**	$Width$ **(°C)**	$Char^a$ **(%)**	$\rho\delta$ **(mg.mm^{-2})**
Untreated thistle	Perkin-Elmer (PE)	214	384	0.200	334	91	32	0.111
	TA Instruments (TA)	206	384	0.180	330	100	35	0.242
	Netzsch (NET)	218	374	0.220	330	92	33	0.250
	Setaram (SET)	219	378	0.200	330	94	34	0.263
	Cahn (Cahn)	226	387	0.165	337	119	34	0.287
	Setaram at 40 °C/min (40)	235	387	0.405	341	91	30	0.278
Untreated beech	Perkin-Elmer (PE)	259	410	0.350	380	58	16	0.121
	TA Instruments (TA)	259	406	0.340	371	56	18	0.250
	Netzsch (NET)	256	404	0.373	378	51	19	0.251
	Setaram (SET)	261	403	0.348	377	48	22	0.286
	Cahn (Cahn)	254	406	0.280	377	58	20	0.327

[a]On dry basis at 550 °C.

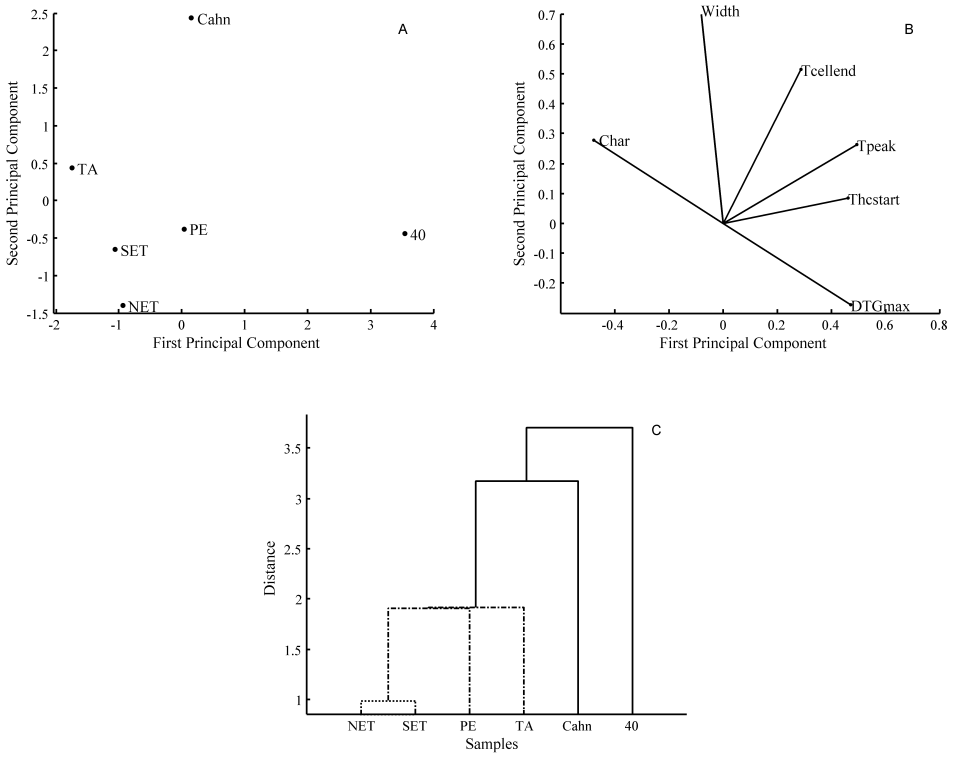

Figure 3.5: Principal Component Analysis from the DTG characteristics of the untreated thistle pyrolysis in different thermogravimetric equipments, under similar experimental conditions: score plot (A), loading plot (B), and dendrogram (C). The first component that has been determined is responsible for 58 % of the total variance, while the second component describes 28 % (see Table 3.6 for the notation of the experiments).

in the PCA calculations. The dendrogram in panel C Figure 3.5 connects similar objects by U-shaped lines. The height of each U represents the distance between the two objects being connected. This corresponds to the Euclidean distances between each pair of observations (Jackson, 2003). In this way, all the above observations are well-identified. Note that the pair formed by the experiments from the Netzsch (NET) and Setaram (SET) thermobalances are the closest linked (dotted line in panel C). Apart from the equivalent experimental conditions, these equipments present the most similar geometric characteristics and furnace configuration. The three-dimensional score plot of the untreated beech results (Figure 3.6) remarks the similarities and differences exposed above.

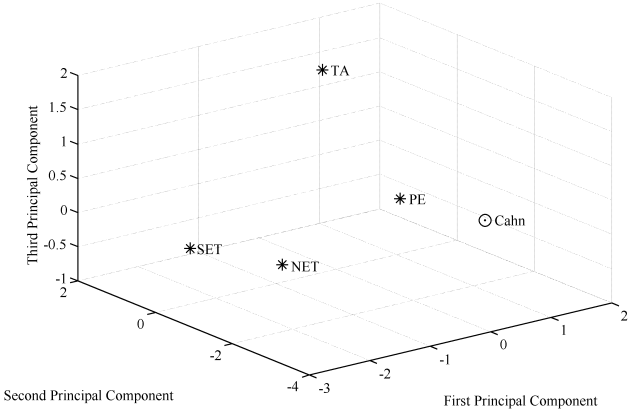

Figure 3.6: Principal Component Analysis from the DTG characteristics of the untreated beech pyrolysis in different thermogravimetric equipments, under similar experimental conditions. The first principal component describes 47 % of the total variance, the second is responsible for 37 % and the third for 10 % (see Table 3.6 for the notation of the experiments).

Given the similarity observed between the Netszch (NET) and the Setaram (SET) results, we calculated new mean DTG characteristics with the data obtained from both thermobalances. These points provide the reference values in tables 3.7 and 3.8, while the rest of results are presented as differences from the references. This is an easy way to quantitatively observe the scattering of the results. The deviations in table 3.7 design the confidence intervals where the means were calculated. In the case of wood these deviations did not exceed the standard deviations from repeated experiments, detailed before.

The experimental curve at 40 °C/min (40) of untreated thistle shifted the reference values, in $T_{hcstart}$ and T_{peak}, by 17 and 11 °C, respectively. For small samples of pure cellulose, Antal and coworkers reported an experimental shift in temperature by about 35 °C, when the heating rate changed from 1 to 10 °C/min (Antal et al., 1998). Finite samples of cellulose are known to undergo endothermic pyrolysis, evoking thermal lags that can dramatically increase with heating rate. Even so, the herbaceous crop appears to be less affected by those heat transfer problems. From the points of view of the current discussion, the work of Stenseng et al. (2001) adds an interesting information to this subject. They observed that a herbaceous biomass sample (straw) presents much lower heat demand than a pure cellulose (Avicel) and, in this way, is less affected by heat transfer intrusions during the experiments.

From a general observation of tables 3.7 and 3.8, for the same heating program, results in the Cahn thermobalance are the most distant to the reference, as predicted

by the PCA analysis. Shifting in T_{peak} is observed by about 7 °C in thistle and 10 °C in wood. The thermogravimetric curves of Avicel cellulose reported by Gronli and coworkers in their round robin study, using instruments under different calibrations, fallen within a range of 17 °C (Grønli et al., 1999). The thermocouple employed in the Cahn thermobalance was not recalibrated for several months prior to this experimentation. The temperature shifts could also result from mass transport limitations. It is possible that the slight differences in the gas flow rates, and the exposure of the sample to the gas flow, might explain some of the observed differences between the different instruments employed in this study.

Small changes in the placement of the thermocouple relative to the sample can also result in shifts of the weight loss curves. Antal et al. reported systematic temperature shifts of 20 - 25 °C at all heating rates in a Dupont 951 TGA, depending upon whether the sample thermocouple was slightly upstream or slightly downstream of the 2-mg cellulose sample (Antal et al., 1998). The TA instrument, the only one in this study with the sample thermocouple above the sample, also entails considerable scattering on the analysis of the thistle samples, mainly for $T_{hcstart}$ and $Width$. Concerning the quantity of char, scattering is also obtained from the use of different apparatus. reported values of solid residue from different instruments spanning a range of 4.0 to 10.9% at 5 °C/min and 2.9 to 10.5% at 40 °C/min (Grønli et al., 1999). In our study, higher variation of solid residue at 550 °C is observed for the wood samples than for the thistle. Decreasing in the layer thickness factor up to 0.15 for thistle and 0.16 for wood in the Perkin-Elmer (PE) instrument, is linked to a char diminishing up to 2 and 7%, respectively.

We included the results with different initial sample masses (between 2 and 13mg), using crucibles with and without a lid, in a second group of PCA evaluations. Figures 3.7 and 3.8 are the results from the untreated and washed thistle calculations, respectively. The corresponding DTG values are presented in table 3.9. It is interesting to observe how the results from both the TA and the Perkin-Elmer (PE) equipments lie further from the rest with different initial sample masses. Note that the latter experiments were only performed in the Netzsch thermobalance. The Perkin-Elmer (PE) layer thickness factor for thistle is close to the one corresponding to an initial mass of 3mg in the the Netzsch analyzer (compare the corresponding $\rho\delta$ values in tables 3.7 and 3.9). However these results appear far from each other in the PCA score plot (see panel A in Figure 3.8) even though the rest of experimental conditions were tried to keep equivalent between both equipments. The characteristics of the originating equipment seems to have a higher influence on the thermal behavior of the samples that certain changes in the experimental conditions in the actual apparatus. All the variables (the DTG points) play a significant role in determining the first principal component (see panel B in Figure 3.8), accounting for the differences from the originating equipment.

The observations that correspond to crucibles with and without a lid appear somewhat differentiated on the second component domain, for which $Char$ and $T_{hcstart}$ have the biggest influence. Employing 9.2 mg of pure cellulose, Antal and coworkers observed a delay in the apparent onset of weight loss by about 40 °C, compared to 0.3-mg results with the same sample under the same heating program (Antal et al.,

Table 3.7: Characteristics of the thermogravimetric curves of thistle from experiments under similar experimental conditions.

Sample and originating equipment			$T_{hc\,start}$ (°C)	$T_{cell\,end}$ (°C)	DTG_{max} (%/s)	T_{peak} (°C)	$Width$ (°C)	$Char^a$ (%)	$\rho\delta$ (mg.mm^{-2})
Untreated	**reference value**		**219**	**376**	**0.210**	**330**	**93**	**34**	**0.257**
	deviations[b]		1	3	0.01	0	1	1	0.01
	differences[c]	PE	-5	8	-0.01	4	-2	-2	-0.15
		TA	-13	8	-0.03	0	7	2	-0.01
		Cahn	8	11	-0.05	7	26	1	0.03
		40	17	11	0.20	11	-2	-3	0.02
Washed	**reference value**		**226**	**397**	**0.253**	**361**	**86**	**26**	**0.256**
	deviations		2	1	0.02	0	3	3	0.02
	differences	PE	-3	8	-0.02	2	2	-1	-0.15
		TA	-17	3	0.00	-1	-14	-1	-0.01
		Cahn	-8	6	-0.05	-4	21	3	0.06
Extracted	**reference value**		**225**	**380**	**0.223**	**339**	**85**	**31**	**0.239**
	deviations		7	4	0.01	1	2	1	0.01
	differences	PE	3	9	0.00	3	-1	-4	-0.12
		TA	4	3	0.00	-1	-1	-1	0.00
Washed and extracted	**reference value**		**225**	**397**	**0.235**	**359**	**87**	**29**	**0.248**
	deviations		1	1	0.01	1	4	2	0.02
	differences	PE	-2	8	0.00	3	-2	2	-0.13
		TA	2	-1	0.00	-2	-3	1	0.01

[a] On dry basis at 550 °C.
[b] Confidence intervals for the reference values estimated from the DTG results in Setaram and Netzsch thermobalances.
[c] Alterations from the reference values.

Table 3.8: Characteristics of the thermogravimetric curves of wood from experiments under similar experimental conditions.

Sample and originating equipment				$T_{hc\,start}$ (°C)	$T_{cell\,end}$ (°C)	DTG_{max} (%/s)	T_{peak} (°C)	$Width$ (°C)	$Char$[a] (%)	$\rho\delta$ (mg.mm^{-2})
Beech	*Untreated*	**reference value**		**259**	**404**	**0.361**	**378**	**50**	**21**	**0.269**
		differences[b]	PE	1	7	-0.01	2	9	-5	-0.15
			TA	1	3	-0.02	-6	6	-3	-0.02
			Cahn	-5	3	-0.08	-1	9	-1	0.06
	Washed	**reference value**[c]		**265**	**406**	**0.388**	**381**	**48**	**20**	**0.288**
		differences	PE	-2	11	-0.01	10	1	-7	-0.16
			Cahn	-4	6	-0.09	16	28	0	0.06
	Extracted	**reference value**[b]		**261**	**406**	**0.360**	**377**	**47**	**22**	**0.280**
		differences	PE	1	4	0.00	5	6	-5	-0.16
	Washed&extracted	**reference value**[b]		**262**	**409**	**0.375**	**381**	**43**	**21**	**0.265**
		differences	PE	6	6	-0.01	6	8	-7	-0.15
Pine	*Untreated*	**reference value**[b]		**253**	**405**	**0.308**	**377**	**69**	**24**	**0.271**
		differences	PE	1	7	-0.01	2	5	-5	-0.15
			Cahn	22	19	-0.07	0	5	3	0.06
	Washed	**reference value**[b]		**261**	**405**	**0.373**	**381**	**53**	**21**	0.277
		differences	PE	1	11	-0.02	6	4	-5	-0.15
			Cahn	10	9	-0.09	16	4	0	0.06
	Extracted	**reference value**[b]		**260**	**401**	**0.335**	**376**	**70**	**24**	**0.267**
		differences	PE	2	9	-0.02	4	0	-4	-0.15
	Washed&extracted	**reference value**[b]		**259**	**404**	**0.365**	**380**	**54**	**22**	**0.264**
		differences	PE	2	12	-0.03	7	5	-4	-0.14

[a] On dry basis at 550 °C.
[b] Alterations from the reference values.
[c] Only from the Setaram thermobalance, since no experiments were performed with this sample in the Netzsch equipment.

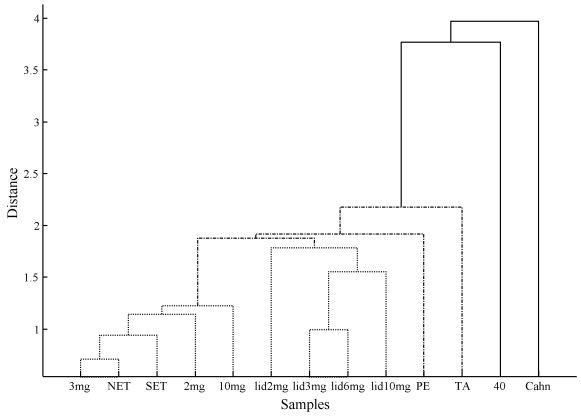

Figure 3.7: Principal Component Analysis from the DTG characteristics of the untreated thistle pyrolysis in different thermogravimetric equipments, under different experimental conditions: dendrogram. The first component that has been determined is responsible for 42% of the total variance, the second component describes 23% and the third 16% (see Table 3.9 for the notation of the experiments).

1998). Besides, the higher-mass DTG curve became much wider. In our case, having increased the initial sample mass of untreated thistle by 8mg, we got a delay in the $T_{hcstart}$ by 8 °C, without using a lid (see table 3.9). The major resistance to the flow of primary volatiles from their vicinity, created by the presence of a pierced lid, also caused a shifting in the onset, for instance, by 7 °C in the 2-mg initial sample mass of the untreated crop. Slightly wider DTG curves, shifted in T_{peak} by maximum 6 °C, are mainly observed for untreated thistle with a lid. All these results are related to heat-transfer and mass-transfer problems by prolonged vapor-phase residence times, as well as temperature inhomogeneities within large samples. Both increase in sample size and presence of a lid result in an increase in the char yield. This is consistent with the fact that the reactive organic vapors produced during pyrolysis evidence a strong propensity to form char when held in the presence of the reacting solid sample (Antal et al., 1998; Mok et al., 1992; Várhegyi et al., 1988a; Antal and Várhegyi, 1995). It is interesting to note that the variations in char yield due to increase in initial sample mass are within the scattering obtained from the use of different apparatus (compare values in tables 3.7 and 3.9).

3.4.2 Influence of the type of sample and pretreatment

After analyzing how the sources and the experimental procedures applied in this thesis affected the results, we introduce in this section general observations on the thermal

Table 3.9: Characteristics of the thermogravimetric curves from experiments in the Netzsch thermobalance, with different initial sample masses, using crucibles with and without a lid

Sample and initial mass[a] (Notation in the Figures)			$T_{hc\,start}$ (°C)	$T_{cell\,end}$ (°C)	DTG_{max} (%/s)	T_{peak} (°C)	$Width$ (°C)	$Char^b$ (%)	$\rho\delta$ (mg.mm^{-2})
Untreated thistle	**without a lid**	2mg (2mg)	225	378	0.200	328	93	31	0.076
		3mg (3mg)	223	375	0.210	329	94	33	0.121
		6mg (NET)	218	374	0.220	330	92	33	0.250
		10mg (10mg)	233	374	0.217	330	91	33	0.391
	with a lid	2mg (lid2mg)	232	383	0.210	334	92	31	0.074
		3mg (lid3mg)	233	382	0.200	334	95	35	0.115
		6mg (lid6mg)	236	381	0.190	333	96	37	0.244
		10mg (lid10mg)	224	379	0.190	335	98	38	0.398
Washed thistle	**without a lid**	2mg (2mg)	225	396	0.250	364	93	25	0.085
		3mg (3mg)	224	398	0.260	363	94	23	0.126
		6mg (NET)	224	396	0.265	361	88	24	0.240
		10mg (10mg)	225	397	0.260	361	89	26	0.398
		13mg (13mg)	228	398	0.260	364	90	26	0.573
	with a lid	2mg (lid2mg)	239	399	0.253	364	89	25	0.082
		3mg (lid3mg)	237	400	0.255	364	85	28	0.118
		6mg (lid6mg)	243	399	0.253	365	87	29	0.252
		10mg (lid10mg)	230	399	0.250	364	84	27	0.421
		13mg (lid13mg)	232	398	0.260	366	90	28	0.583

[a] Rough sample amounts.
[b] On dry basis at 550 °C.

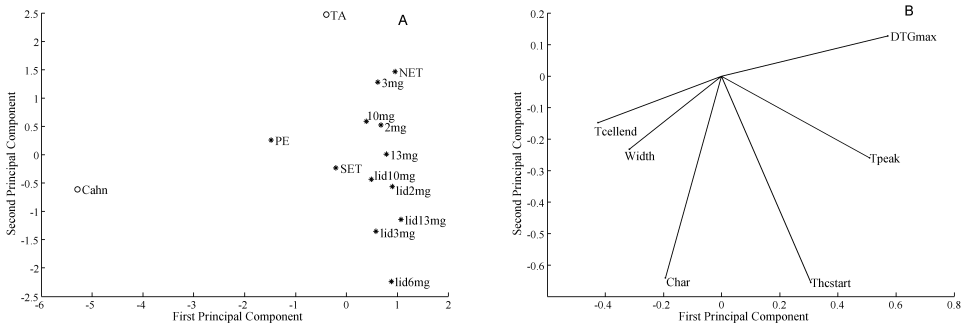

Figure 3.8: Principal Component Analysis from the DTG characteristics of the washed thistle pyrolysis in different thermogravimetric equipments, under different experimental conditions: score plot (A), and loading plot (B). The first component that has been determined is responsible for 46% of the total variance, the second component describes 25% and the third 15% (see Table 3.9 for the notation of the experiments).

decomposition of all the samples under study, so as to comprehend the differences produced by the type of sample and pretreatment. These observations will help the reader in following the exposition in the next chapters. Given the varied source of results and the non-negligible scattering observed in the section before, we needed to select a reliable set of DTG values in order to characterize the thermal behavior of the entire pool of samples. Accordingly, we considered the mean values from the Setaram and Netzsch thermobalances that served as the reference in the analysis of the equivalent experimental conditions (tables 3.7 and 3.8).

The herbaceous crop decomposes over the widest temperature range (PW), exhibiting the smallest rates of decomposition, the lowest T_{peak}, and the highest quantities of carbonaceous residue ($char$) among the studied samples. The $T_{hcstart}$ values give evidence that the devolatilization of this sample starts at lower temperatures than those of the woody species. The two wood samples reveal a roughly similar thermal behavior, although some differences can be observed. The shoulder at about 330 °C is more discernible in the case of the beech sample, which has the highest rate of decomposition and the lowest char yield.

Some of the DTG curves are compared in Figure 3.9. The pretreatments have a more pronounced effect on the thistle than on the wood samples, owing to the higher mineral matter and extractive content of the herbaceous sample (8.10% ash and 6.1% extractives in thistle versus 0.24 - 1% and 1.15 - 4.85% respectively in wood). The water-washed samples show clearly different thermal characteristics from the original ones, whereas the extraction changes the devolatilization of the samples only to a smaller extent. The decomposition of the water-washed samples is displaced towards higher temperatures, taking place at higher rates and with a smaller amount of char

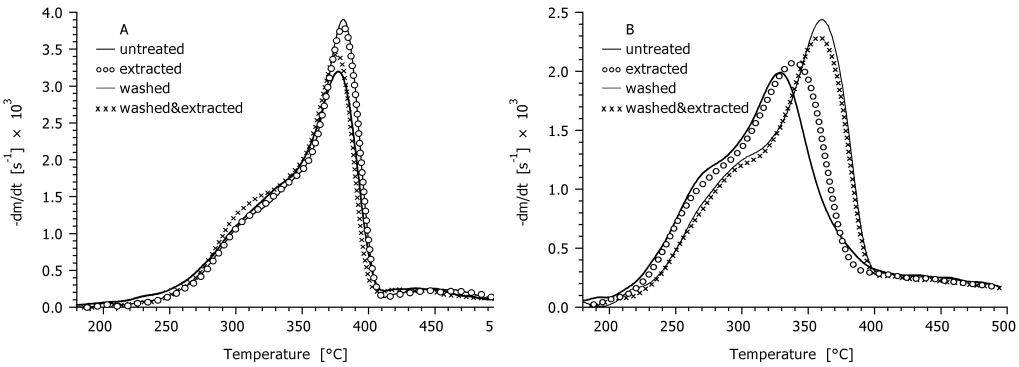

Figure 3.9: DTG curves of untreated and pretreated pine (A) and thistle (B) samples at 20 °C/min in the Setaram thermobalance. [A.1.3]

formed than in the case of the untreated and extracted samples.

Figure 3.10 panel A shows the score plot resulting from the PCA calculation based on the DTG characteristics of all the samples under study. The first component that has been determined is responsible for 93 % of the total variance, while the second component describes 5 %. The contribution of the other principal components is negligible. The untreated and extracted herbaceous crop (UT and ET, respectively) appear clearly separated from the wood, whereas the points corresponding to the wood samples lie much closer to one another. Thistle gets closer to the wood samples after washing (WT and WET points) implying that the thermal behaviour of these samples is more similar to that of the wood samples. Another distinction can be recognised from the different pretreatments: the extracted samples lie much closer to the untreated ones than to the rest of pretreated samples (Note that the scales of the x and y axis are different). This observation is more evident in the case of thistle. The water-washing pretreatment also makes the pine and the beech approach one another, decreasing the scattering observed within the group of non-washed samples of wood. All these observations evidence the important role of the inorganic content (Várhegyi et al., 1989b; Shafizadeh, 1985; DeGroot and Shafizadeh, 1984; Pan and Richards, 1989), and reaffirm the more pronounced effect of water-washing than extraction on the thermal behaviour of wood and thistle.

All the above described groups are well-identified in the dendrogram (Figure 3.10 panel B). Note that the pairs formed by the non-washed (ie. untreated and extracted) samples of thistle and pine show the largest distances. This result can be connected with their higher amount of mineral matter and extractives among the studied samples.

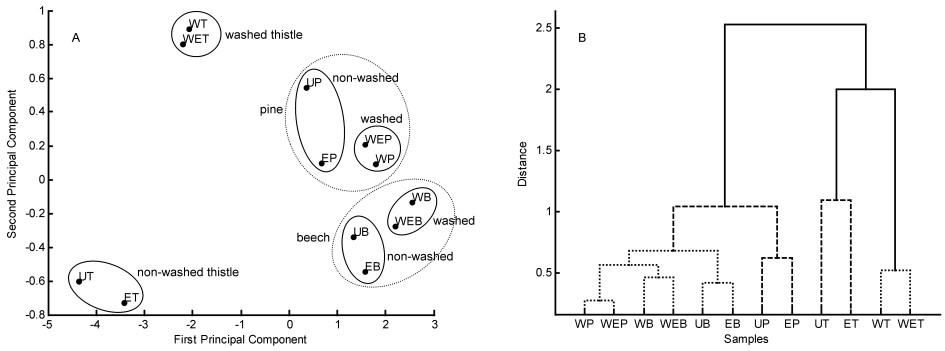

Figure 3.10: Principal Component Analysis from the DTG Characteristics of the entire set of thermogravimetric curves: (A) score plot, and (B) Dendrogram. (see Table 3.10 for the notation of the samples). [A.1.2]

Table 3.10: Types of sample and their notation in the figures

Abbreviation	Description
UT	Untreated thistle
WT	Washed thistle
ET	Extracted thistle
WET	Washed and extracted thistle
UP	Untreated pine
WP	Washed pine
EP	Extracted pine
WEP	Washed and extracted pine
UB	Untreated beech
WB	Washed beech
EB	Extracted beech
WEB	Washed and extracted beech

3.5 Conclusions of this chapter

In this chapter, it is introduced and described the entire thermogravimetric system used in this thesis. It concerns investigations on the thermal behavior of three biomass materials (pine and beech from carpentry residues and thistle from an energy plantation), within the range of slow pyrolysis, including various pretreatments to eliminate inorganic matter and extractives. The thermogravimetric curves obtained in several apparatus are characterized from a quantitative point of view, based on the definition of characteristic reaction temperatures, devolatilization rates, and mass fractions.

Chemometric evaluations (PCA calculations) of the DTG characteristics values revealed significant effect of the TGA apparatus on the thermal behavior of the samples. Results from experiments performed under roughly equivalent experimental conditions in different instruments evidenced non-negligible scattering. Apart from the well-known influence of mass and heat transport limitations in the sample crucible, both the geometry and the configuration of the furnace appear to have an important effect. The slight different gas velocities, the way that the sample is shelter due to the sensitiveness of the instrument, and changes in the placement of the thermocouple relative to the sample, might explain some of the observed differences between the results from different instruments employed in this study. Some experimental procedures, like temperature calibration and scarcity in data collection, are also key factors. Different initial sample masses in an apparatus did not imply a bigger scatter than that from the use of different thermobalances. On the whole, the observed shifting in temperatures and masses did not exceed reported scattering on the pyrolysis of pure cellulose.

Finally, we observed the effect of the type of sample and pretreatment with the help of a further PCA calculation. Differences in the degradation dynamics between the samples obeyed to the variable amounts and nature of the main components. The experimental results corroborated the catalytic effect of the inorganic matter present in the biomasses and the influence of the lignin and extractive degradation characteristics. The water-washing pretreatment made the thermal behavior of thistle more similar to those of the wood samples. The effect of the extraction was evidenced to a smaller extent.

Chapter

FOUR

Primary decomposition. Kinetic study

In this chapter, various kinetic approaches are employed in order to determine the best kinetic parameters that describe the primary pyrolysis experiments analyzed in the chapter before, under different heating programs. After determining separate kinetic parameters for each of the samples, a further check on the pretreatments effect is carried out by testing how a common set of activation energies describes the untreated and pretreated samples of the same feedstock, as well as the experiments coming from different thermoanalyzers under equivalent experimental conditions. Most of the results and discussion in this chapter have been already published in papers A.1.3[1] and A.1.4[2].

4.1 Kinetic Modeling of Thermal Decomposition

4.1.1 The Model of Pseudocomponents

The non-isothermal thermogravimetric analysis of the biomass materials provides more or less overlapped peaks for the cellulose and hemicellulose components while the lignin and the extractives contribute to the mass loss in wider temperature domains. An inherent difficulty exists in the deconvolution of the DTG curves due to the high variability of these compounds from one biomass species to another. A practical way for the mathematical description is the assumption of pseudocomponents formed by fractions of the biomass components decomposing in similar way in similar temperature ranges. For each pseudocomponent, a conversion (reacted fraction) α_j and a reaction rate, $d\alpha_j/dt$ are defined. (See the "Nomenclature" Chapter for symbols and subscripts.) The overall reaction rate is a linear combination of these partial reactions:

[1] Gómez, C. J., Várhegyi, G., Puigjaner, L., 2005.
[2] Gómez, C. J., Manyà, J. J., Velo, E., Puigjaner, L., 2004.

$$dm^{calc}/dt = -\sum_{j=1}^{M} c_j d\alpha_j/dt \tag{4.1}$$

where, M is the number of the pseudocomponents and c_j is the fraction of the overall mass loss due to the jth pseudocomponent. Each partial reaction is approximated by an Arrhenius equation:

$$d\alpha_j/dt = A_j exp(-E_j/RT)(1-\alpha_j)^{n_j} \tag{4.2}$$

Here A_j is the preexponential factor, E_j is the apparent activation energy, and n_j is the reaction order.

4.1.2 Evaluation by the Method of Least Squares

The following evaluation strategies to obtain the best-fit kinetic parameters, using least squares non-linear methods, are examined and compared:

- Optimization algorithms to minimize the fit error, defined by a function related with the difference between the experimental and the simulated TG weight loss curve (integral form) or DTG differential curve (differential form).
- Description of the global decomposition by different number and type of pseudocomponents and nth order kinetics for the partial reactions.
- Simultaneous evaluation of experiments under different heating programs.
- Kinetic description by the same set of activation energies, for experiments with samples subjected to different pretreatments, coming from different thermoanalyzers.

When the integral form of the objective function was used, we evaluated one experiment simultaneously by minimizing the following sum:

$$S = \sum_{i=1}^{N} \left(m^{obs}(t_i) - m^{calc}(t_i)\right)^2 /N \tag{4.3}$$

where t_i denotes the time values in which digitized sample mass values (m^{obs}) were taken, and N is the number of the t_i points considered in the evaluation.

Using the DTG differential curves, we determined the unknown parameters of the model by the simultaneous evaluation of one or more than one experiment for each sample:

$$S = \sum_{p=1}^{N_{exp}} \sum_{i=1}^{N_p} \left[\left(\frac{dm}{dt}\right)_p^{obs}(t_i) - \left(\frac{dm}{dt}\right)_p^{calc}(t_i) \right]^2 /N_p/h_p^2 \tag{4.4}$$

Subscript p indicates the heating programs. N_{exp} is the number of experiments evaluated simultaneously. t_i denotes now the time values in which digitized $(dm/dt)^{obs}$

values were taken, and N is the number of the t_i points in a given experiment. h_p denotes the heights of the evaluated curves [$h_p = max(-dm/dt)_p^{obs}$]. The division by h_p serves for normalization.

If the objective function in its integral form is chosen, the data collected in the apparatus does not need more treatment, and can be used almost as they were collected. However the weight fraction curves are not very sensitive to processes that can superpose partially or even go unnoticed. The differential objective is much more sensitive to these changes but care must be taken in the calculation of the derivative because small experimental errors or deviations can produce large errors with respect to the actual derivative curve (Conesa et al., 2000). In this work, the DTG curves were determined by spline smoothing (Várhegyi and Till, 1999). In most of the cases, the root mean square difference between the TG curves and the smoothing splines was small, 0.5 μg ($\approx$ 0.01%), accordingly the differentiation itself did not introduce considerable systematic error into the evaluation. In the case of the experiments coming from the Cahn thermobalance, however, the higher sparse data produced a difference 10 times bigger.

For each group of experiments evaluated simultaneously a fit quantity was calculated:

$$fit(\%) = 100(S/N_{exp})^{-1/2} \tag{4.5}$$

When the fit for a single experiment is given, the same formula is used with $N_{exp} = 1$. Similar formulas can be used to express the repeatability of the experiments in quantitative form. In this case, the mean square root difference between two repeated experimental DTG curves is calculated and normalized by the peak maximum. In this way we got an average relative error of 1% for the repeatibility of the non-isothermal experiments.

MATLAB 6.0, FORTRAN 90 and C++ programs are used as the simulation tool. The latter two programs were developed by G. Várhegyi (Várhegyi et al., 1989a, 1988a; Antal et al., 1998; Várhegyi et al., 1997; Grønli et al., 2002; Mészáros et al., 2004b). In the MATLAB program, the differential equations are solved by a variable-order method (stiff problems solver, (Shampine and Reichelt, 1997)). The minimum fit is determined by a Nelder-Mead direct search method (Lagarias et al., 1998). For the FORTRAN 90 and C++ programs, the differential equations of the model are solved by a high precision (10^{-10}) numerical solution. The least-squares parameters are determined by a modified Hook-Jeeves minimization, which is a safe and stable direct search method. Each minimization was repeatedly restarted from the optimum found in the previous run of the algorithm until no further improvement was achieved. The general data processing and graphic programs developed by G. Várhegyi were used in many of the figures and data processing steps in several points of the thesis.

4.2 Results and Discussion

4.2.1 Model assuming three partial reactions

The starting point for the kinetic analysis performed in this thesis was the evaluation of the predictive capacity of the revisited summative model previously proposed by the UPC laboratory (Manyà et al., 2003), in the thermal decomposition of the main set of samples under study (untreated and water-washed pine, beech and thistle). The model contemplates three biomass pseudocomponents through application of the addition principle (Antal and Várhegyi, 1995). The approach is based on the assumption of a one-stage process with first-order reaction for each pseudocomponent. There is an exception for the third partial reaction (linked to lignin), for which a third-order reaction is used. This model was previously applied for the kinetic evaluation of sugarcane bagasse and waste wood samples, coming from an heterogeneous source and with a considerable amount of mineral matter and extractives (Manyà et al., 2003). Despite this, predictions from the model reproduced correctly the experimental TG curves. These results justified the interest in applying the same model to describe the global mass loss during pyrolysis of other biomasses of practical interest.

In a first calculation of the unknown kinetic parameters, we considered the fit to the TG curves (Equation 4.3). In Figure 4.1, Experimental TG and DTG curves of some of the samples are compared with the resulting simulated curves. Kinetic parameters obtained from the experiments performed in the Cahn thermobalance are presented in table 4.1. The description of the pseudocomponents is as follows: (1) a hemicellulose fraction that decomposes in the low-temperature range (first peak of the DTG curve); (2) a cellulose fraction that decomposes in the mid-temperature range (second peak of the DTG curve); (3) the fraction of lignin present plus extractives and the remaining amounts of holocellulose.

Apparently, successful prediction of the global mass loss process was achieved, from the observation of the TG curves (see panels A, Figure 4.1). However, when we used the parameters showed in table 4.1 to calculate the simulated DTG curves, unsatisfactory fits to the experimental data were observed (see panels B in Figure 4.1), mainly in the case of thistle. Volatile production is overestimated on the shoulder and peak of hemicellulose and cellulose decomposition, respectively. Besides, some underestimation is observed in between, as if another partial reaction was missing.

The parameters corresponding to the second pseudocomponent in table 4.1 fall into the range usually referred to in the literature for cellulose (activation energy value of 244 $\pm$ 10 kJ/mol and preexponential factor logarithmic value of 19 $\pm$ 1 s^{-1}, (Antal and Várhegyi, 1995; Grønli et al., 1999). For the first pseudocomponent, the parameters obtained are of order similar to those published by Manyà et al. (2003) using the same model, mainly in the case of the woody samples.

In the attempt to get a better approach to the subtle changes in the mechanism, we evaluated the fit to the DTG curves (Equation 4.4) in a further calculation. The adjustment obtained to the differential weight loss curve improved considerably (see Figure 4.2), without a serious compromise of the TG fit. Nevertheless, some of the partial reaction showed strange areas and positions. In other words, they appeared as

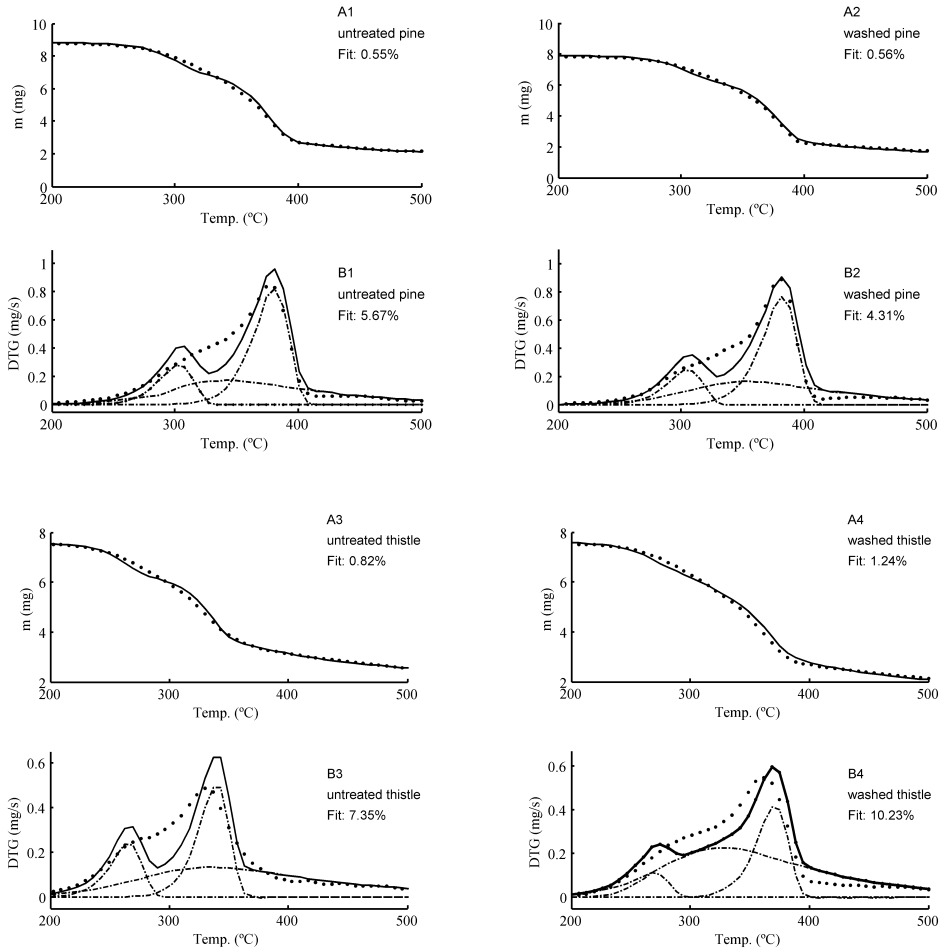

Figure 4.1: TG (A) and DTG (B) curves during pyrolysis of the untreated and water-washed pine and thistle samples at 20ºC/min in the Cahn thermobalance. The symbols (o) are experimental data. The solid line curves are predictions from employing a three partial reactions (-.-) model. Corresponding kinetic parameters obtained by evaluating the TG curves (integral form).

Table 4.1: Results of the Evaluation by employing the three partial reactions model

		pseudocomponent			
		1	2	3	TG fit (%)
untreated pine	$\log A$ (s^{-1})	15.69	18.01	5.67	0.55
	E (kJ/mol)	194.35	243.79	93.66	
	c	0.12	0.30	0.33	
	n	1	1	3	
washed pine	$\log A$ (s^{-1})	15.60	18.01	5.66	0.56
	E (kJ/mol)	196.66	245.22	92.60	
	c	0.12	0.36	0.32	
	n	1	1	3	
untreated beech	$\log A$ (s^{-1})	15.68	18.01	5.48	0.53
	E (kJ/mol)	196.65	243.69	90.03	
	c	0.20	0.35	0.32	
	n	1	1	3	
washed beech	$\log A$ (s^{-1})	15.67	18.01	5.83	0.51
	E (kJ/mol)	196.85	245.32	95.00	
	c	0.13	0.38	0.29	
	n	1	1	3	
untreated thistle	$\log A$ (s^{-1})	15.68	19.01	3.24	0.82
	E (kJ/mol)	183.24	239.68	57.84	
	c	0.14	0.17	0.44	
	n	1	1	3	
washed thistle	$\log A$ (s^{-1})	15.63	19.04	4.72	1.24
	E (kJ/mol)	184.74	248.35	79.69	
	c	0.09	0.21	0.43	
	n	1	1	3	

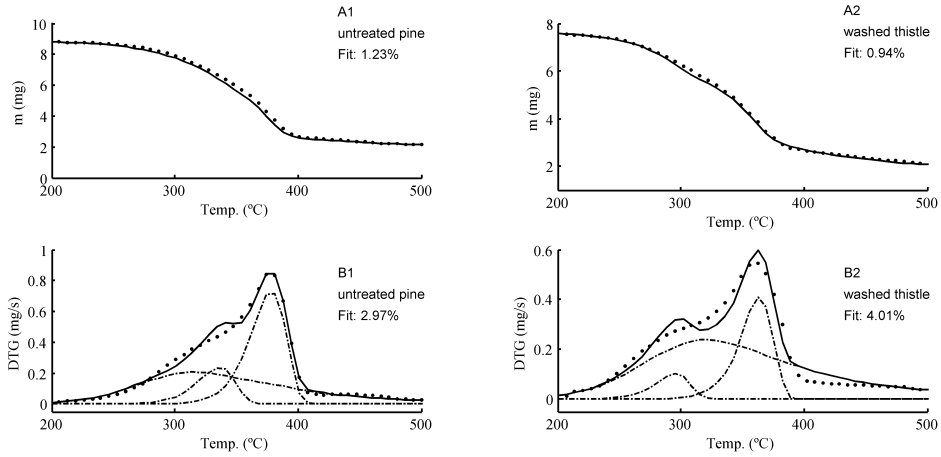

Figure 4.2: TG (A) and DTG (B) curves during pyrolysis of the pine and thistle samples at 20°C/min in the Cahn thermobalance. The symbols (o) are experimental data. The solid line curves are predictions from employing a three partial reactions (-.-) model. Corresponding kinetic parameters obtained by evaluating the DTG curves (differential form).

flat and ill-defined peaks. The partial curves of the pseudocomponents associated to hemicellulose and lignin decomposition (1 and 3, respectively) were forced to overlap each other so as to compensate the volatiles production from 300 to 350 °C.

In view of the troubles found in these calculations, we contemplated tasting the kinetic approximation by employing more than three partial reactions, according with previous studies that report more than one peak to define extractives and hemicellulose decomposition (Mészáros et al., 2004b; Várhegyi et al., 1997; Di Blasi and Lanzetta, 1997). In the following sections, we will also involve the experiments subjected to a stepwise heating program (see Section 3.2.5) in the determination of the kinetic parameters, in order to increase the information content from the experiments, as well as providing a more accurately description of the temperature dependence of the corresponding reaction rates. In addition, we will observe how the asymmetry on the peak shapes, produced by the use of third order reactions, can affect the description of the global decomposition.

4.2.2 Model assuming first-order kinetics

In a next calculation, we simultaneously evaluated the experiments under both linear (20°C/min) and stepwise heating programs (Equation 4.4), looking for the number of partial first-order reactions that best described the DTG curves. The source of this set of evaluated experiments was the Setaram thermobalance. Note that both temper-

ature programs belong to the range of slow pyrolysis in this study. Accordingly, the same kinetics and mechanism were assumed for both type of experiments. The partial curves and the individual fit between the experimental and simulated DTG curves are shown in Figure 4.3 for a selection of the experiments. In the present work four or five reactions, depending on the sample, were necessary to describe well the characteristics of the observed DTG curves. The complete characterization of the untreated pine decomposition involved one additional partial reaction in the low temperature region (around 250 °C), while the other samples did not reveal considerable mass loss in this range. The parameters obtained and fit values for the untreated and washed samples are summarized in Table 4.2. As the results show, the stepwise and the linear heating rate experiments can be described by the same kinetic parameters, indicating that the higher heat flux demand of the linear $T(t)$ experiments did not result in significant heat transfer problems. Based on the very broad decomposition range of the lignin (Grønli et al., 2002) and extractives (DeGroot et al., 1988), contribution from these components are expected to all partial peaks. The first domain obtained for untreated pine corresponds mainly to the thermally labile functional groups of extractives and hemicellulose, in agreement with the high extractives content in this sample. The next peaks around 300 °C and 330 °C are dominated by the main hemicellulose decomposition, in accordance with other works reporting double hemicellulose peaks on the DTG curves of lignocellulosic materials, as referenced before. The sharp, high peak around 370 °C is characteristic of the cellulose pyrolysis. The last peak, around 440 °C, corresponds mainly to lignin thermolysis (Grønli et al., 2002; Jakab et al., 1997, 1995). The thistle sample differed from the woods. (See panel C Figure 4.3) It can be due partly to the chemical differences between the constituents of an herbaceous plant and a wood, and partly to the much higher ash content. The effect of the mineral matter is well reflected by the lower overlapping of the partial peaks on the water-washed thistle, as shown in panel D of Figure 4.3.

The resulting kinetic parameters are close to the ones presented by Teng et al. for the cellulose and hemicellulose components in the pyrolysis of untreated rice hulls (Teng and Wei, 1998; Teng et al., 1997), as well as those obtained by Mészáros et al. (2004b) for short rotation forest biomass. It is interesting to note that higher activation energies for the cellulose decomposition, like in the previous section, are more frequently reported in the literature (Antal and Várhegyi, 1995; Grønli et al., 1999). The lower cellulose activation energies obtained in the present part of the work may be due to several factors. The involvement of the stepwise temperature program requires values that describe the decomposition in a broader range of experimental conditions. Chemical or physical inhomogeneities in the cellulose components may also lead to a broader temperature domain. From a mathematical point of view, broader DTG peaks can be described by lower E values. Besides, there is a variation in the activation energies for different, pure cellulose samples, too, even if they are determined at identical experimental conditions by the same evaluation techniques (Antal et al., 1998). The lowest activation energy reported for a pure cellulose by Antal et al. is close to the results of the present work.

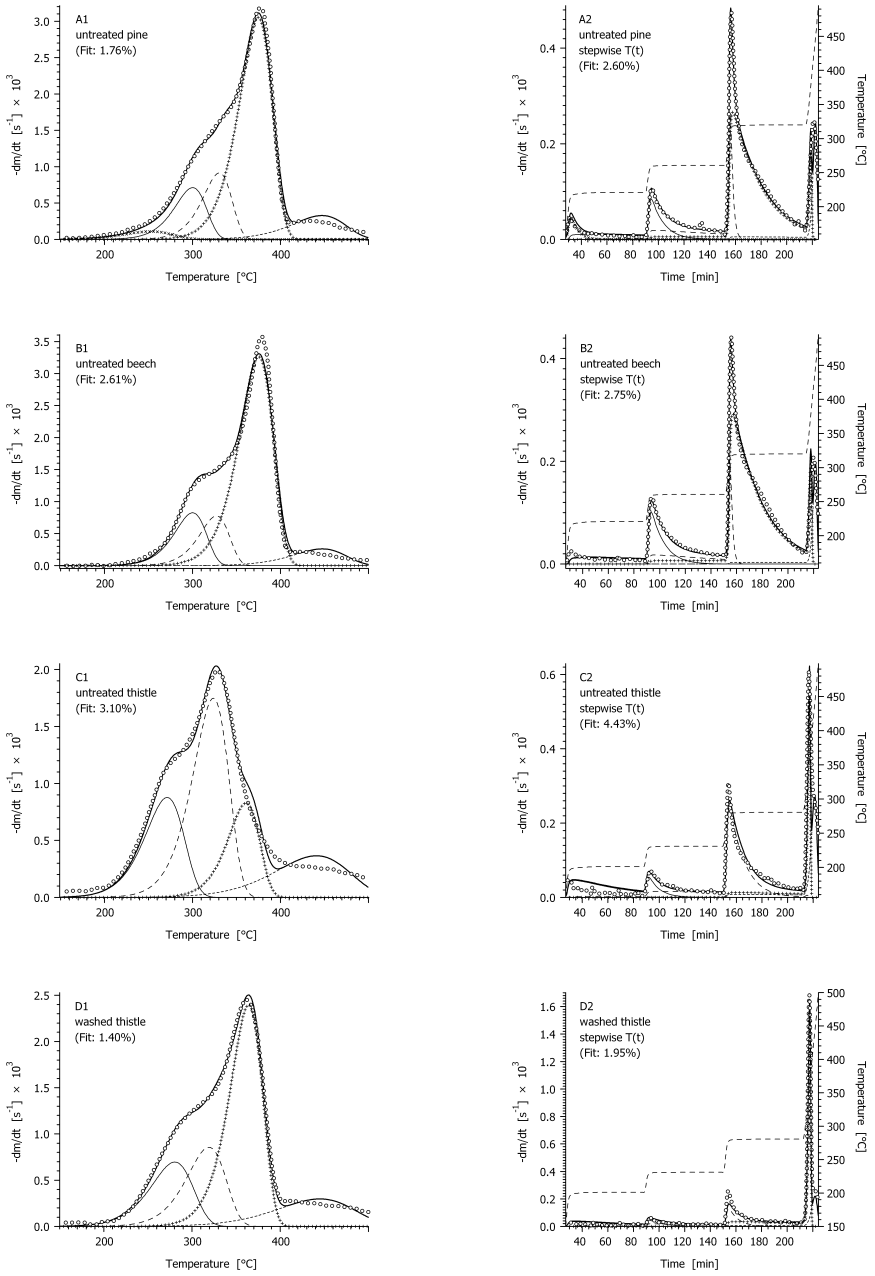

Figure 4.3: Comparison between observed (o o o) and simulated (—) DTG curves at 20 °C/min (1) and at a stepwise temperature program (line - - - in panel 2) employing the first-order model with more than three partial reactions (see Table 4.3 for the description of the simulated partial reactions).

Table 4.2: Results of the evaluation by the first-order model with more than three partial reactions

		pseudocomponent					
		i[a]	1	2	3	4	fit[b] (%)
untreated pine	log$A$ (s^{-1})	5.73	11.86	13.95	12.96	7.96	2.18
	E (kJ/mol)	77	149	181	183	137	
	c	0.02	0.10	0.12	0.45	0.08	
washed pine	log$A$ (s^{-1})		11.80	14.35	13.50	7.65	3.23
	E (kJ/mol)		148	185	190	134	
	c		0.10	0.11	0.50	0.07	
untreated beech	log$A$ (s^{-1})		11.72	13.67	12.58	8.22	2.68
	E (kJ/mol)		148	177	178	140	
	c		0.12	0.10	0.49	0.06	
washed beech	log$A$ (s^{-1})		12.12	14.17	13.02	8.29	4.04
	E (kJ/mol)		153	183	185	142	
	c		0.12	0.09	0.52	0.05	
untreated thistle	log$A$ (s^{-1})		8.67	10.86	13.51	4.85	3.77
	E (kJ/mol)		109	145	185	95	
	c		0.15	0.28	0.12	0.12	
washed thistle	log$A$ (s^{-1})		7.57	9.34	13.20	4.52	1.68
	E (kJ/mol)		100	127	182	92	
	c		0.13	0.15	0.34	0.10	

[a] A low temperature process observed at the untreated pine sample.
[b] Overall DTG fit on the simultaneous evaluation of both linear and stepwise heating experiments.

Table 4.3: Partial curves in the kinetic decomposition and their notation in the figures

Name and description	Representation
i: Thermally labile groups of extractives, hemicellulose, and lignin	x x x
Pseudocomponent 1: First main peak of hemicellulose (+ some devolatilization of extractives and lignin)	——
Pseudocomponent 2: Second main peak of hemicellulose (+ some devolatilization of extractives and lignin)	– – –
Pseudocomponent 3: Cellulose peak (+ some devolatilization of extractives and lignin)	+ + +
Pseudocomponent 4: Lignin's main peak	- - -

4.2.3 Model assuming third-order kinetics for the last pseudocomponent

The result of Manyà et al. (2003) shows that a better fit can be achieved if the behavior of the last pseudocomponent, dominated by the lignin decomposition, is described by a 3rd order reaction. This observation has been deduced from the evaluation of constant heating rate experiments. The present evaluation extends this result to the simultaneous evaluation of experiments with linear and stepwise temperature programs. The parameters and fits obtained by assuming $n_4 = 3$ are shown in Table 4.4 and Figure 4.4. The highest improvement appeared in the fit of the thistle sample. The kinetic parameters of the last pseudocomponent were obviously changed, while the rest of the parameters were only slightly affected. The E_4 values obtained for thistle are close to the corresponding values of Mészáros et al. (2004b) who used $n = 2$ in their nth order model. For the wood component, however, much higher E_4 values were obtained than those reported formerly in the literature. Keeping in mind that this pseudo component describes the high temperature processes of the biomass decomposition, and higher decomposition temperatures are usually due to higher energy barriers, the values obtained in the present work may be closer to the true physical activation energies of these reactions than the values obtained from linear temperature programs only.

4.2.4 Prediction by the model to a higher heating rate

A simple way to check the reliability of a model is to study how suitable it is to predict phenomena outside the domain used in the determination of its parameters. For this reason, we tested how the results obtained from the stepwise and the 20 °C/min experiments can predict the behavior of the samples at a higher heating rate, 40 °C/min. This sort of experiments evidenced the biggest variation in DTG characteristics from the PCA evaluation in the chapter before. An acceptable fit was obtained in this case, as shown in Figure 4.5, indicating the strength of the approaches used in our work.

This sort of tests has rarely been used in the least squares evaluation of the thermoanalytical curves of biomass materials. Várhegyi et al. (2002) predicted the behavior of stepwise heating programs from the results of 10 and 40 °C/min experiments in a charcoal study. Conesa et al. (2000) emphasized the importance of describing experiments with different temperature programs with exactly the same kinetic parameters as a method for distinguishing a robust model.

Several other works stated, however, that high-heating rate experiments cannot be described by the kinetic parameters obtained from lower heating rate ones due to heat transfer problems (Antal et al., 1998; Mészáros et al., 2004b; Várhegyi et al., 2001; Chornet and Roy, 1980; Antal and Várhegyi, 1995; Narayan and Antal, 1996; Várhegyi et al., 1989a). In these investigations both the sample and the equipment differ from the ones employed in the present work (referred to the Setaram thermobalance in the present evaluation). Besides, the quoted works, with the exception of Mészáros et al. (2004b), were based only on linear heating rate experiments. Concerning the

Table 4.4: Results of the evaluation by assuming $n_4 = 3$

		pseudocomponent					
		i	1	2	3	4	fit (%)
untreated pine	$\log A$ (s^{-1})	5.82	11.88	14.07	13.01	14.14	1.69
	E (kJ/mol)	78	150	182	183	215	
	c	0.02	0.10	0.11	0.46	0.08	
	n	1	1	1	1	3	
washed pine	$\log A$ (s^{-1})		11.81	14.43	13.53	16.18	3.04
	E (kJ/mol)		149	186	190	244	
	c		0.10	0.11	0.50	0.07	
	n		1	1	1	3	
untreated beech	$\log A$ (s^{-1})		11.78	13.71	12.64	16.08	2.37
	E (kJ/mol)		148	177	179	241	
	c		0.12	0.10	0.50	0.06	
	n		1	1	1	3	
washed beech	$\log A$ (s^{-1})		12.16	14.21	13.04	20.89	3.83
	E (kJ/mol)		153	183	185	307	
	c		0.12	0.09	0.53	0.05	
	n		1	1	1	3	
untreated thistle	$\log A$ (s^{-1})		8.82	11.05	14.77	8.75	3.11
	E (kJ/mol)		111	146	197	138	
	c		0.15	0.26	0.11	0.16	
	n		1	1	1	3	
washed thistle	$\log A$ (s^{-1})		7.63	9.57	13.34	7.72	1.43
	E (kJ/mol)		101	130	184	130	
	c		0.14	0.15	0.33	0.14	
	n		1	1	1	3	

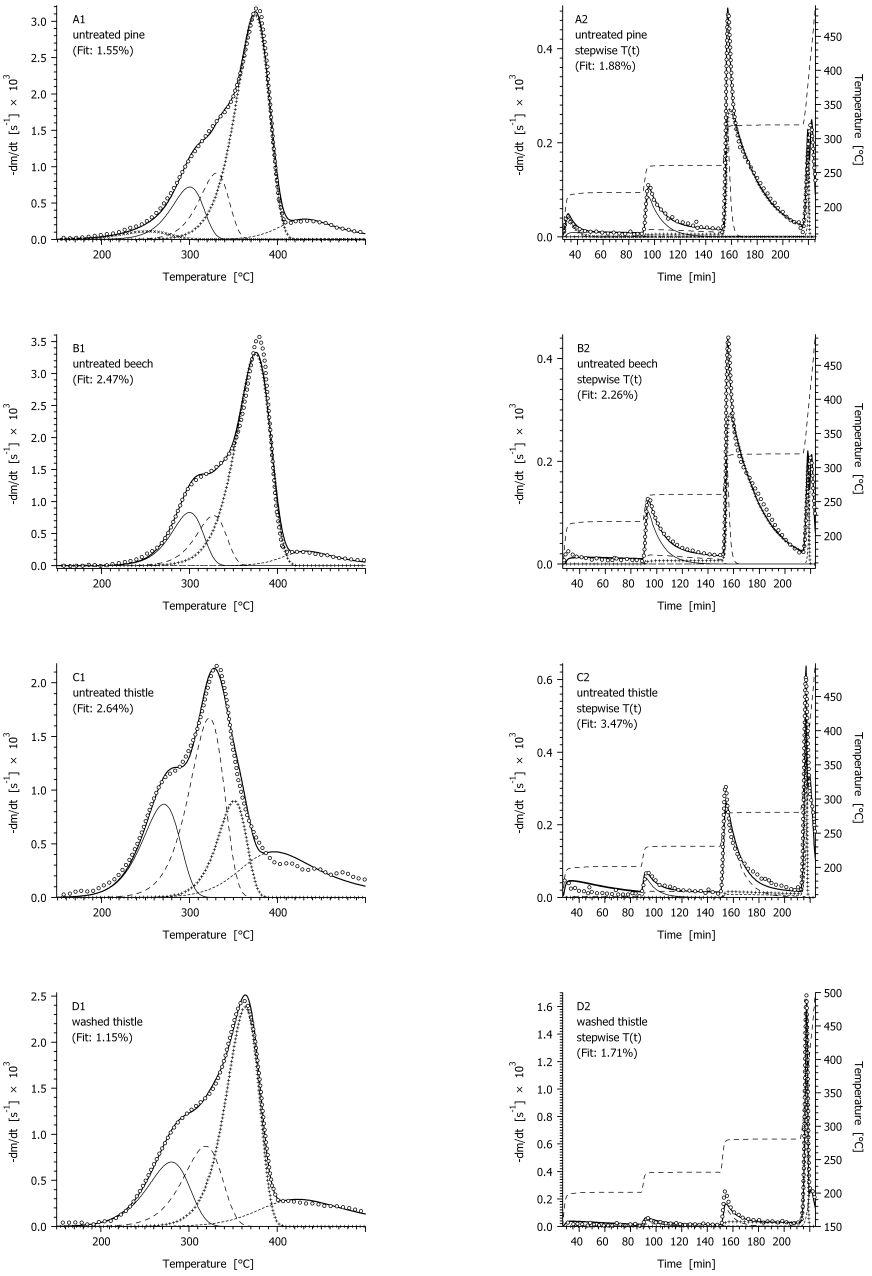

Figure 4.4: Comparison between observed (o o o) and simulated (—) DTG curves at 20 °C/min (1) and at a stepwise temperature program (line - - - in panel 2) employing third-order reaction for the last pseudocomponent (see Table 4.3 for the description of the simulated partial reactions).

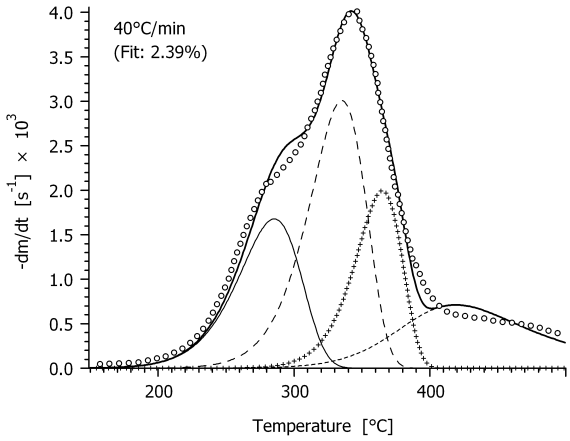

Figure 4.5: Comparison between the observed (o o o) and simulated (—) DTG curves for untreated thistle at 40 °C/min employing third-order reaction for the last pseudocomponent and the same resulting kinetic parameters at 20 °C/min.

samples, the work of Stenseng et al. (2001) adds an interesting information to this subject. They observed that a herbaceous biomass sample (straw) presents much lower heat demand than a pure cellulose (Avicel) and, in this way, is less affected by heat transfer intrusions during the experiments.

4.2.5 Describing the experiments by the activation energies of the water-washed samples

Experiments coming from the Setaram thermobalance

As described earlier, we studied the thermal decomposition of untreated, water-washed, and ethanol-extracted samples as well as samples submitted to both water-washing and ethanol extraction, from experiments performed in different thermoanalytical equipments. During the kinetic evaluation of these experiments we looked for an approach that emphasizes the similarities between the differently treated samples while expressing the differences in quantitative form, in terms of the kinetic parameters. Taking into account the results of previous works (Várhegyi et al., 2004), we employed the same set of activation energies for the pretreated and the untreated versions of a given sample with varying preexponential factors and c_j coefficients. This approach can be visualized as follows. For non-isothermal experiments an activation energy value approximately defines the width of the corresponding partial peak while the main effect of a small variation in the corresponding log A is the shifting of the temperature domain of the given peak. The variation of the c_j coefficients reflects the change of the volatile matter production of the pseudocomponents. They are nearly

proportional to the height of the curves when the E values are fixed and the log A values show only a limited variation.

We obtained favorable results by employing the activation energies of the water-washed experiments. Water washing does not considerably alter the chemical integrity of the sample (Antal and Várhegyi, 1995; Mészáros et al., 2004a; Teng and Wei, 1998), and offers a better procedure for separating peaks than other pretreatments. The results for the experiments coming from the Setaram thermobalance are summarized in Table 4.5. The fit between the simulated and observed data are illustrated by Figures 4.6 and 4.7. In Table 4.5, the kinetic evaluation of the water washed samples provided the reference values. In the other cases, the alterations from the corresponding reference values are given to provide an easy view on the differences between the water-washed and the other samples. Due to the repetition of several experiments, each value in Table 4.5 was deduced from 2 - 6 experiments. An additional evaluation of the untreated thistle sample under 40 °C/min linear heating rate by the actual method has also been included for comparative purposes. The log A and c_j parameters were formed by averaging while the fits are the root-mean-square values of the corresponding experiments, as defined by equation 4.5.

It is interesting to note that using the activation energies of the water-washed experiments resulted only in slight alteration of the fit values. In the case of the wood samples, only the c_3 coefficient revealed a considerable variation while the rest of the parameters showed only minor changes. c_3 expresses mainly the volatile formation from the cellulose component. Its values were lower by a factor of about 0.9 in the untreated wood samples indicating the catalytic activity of that part of the mineral content which can be removed by water-washing. The lower c_3 values correspond to a higher char formation from the cellulose component of the untreated samples.

The corresponding values of the untreated and extracted samples were similar, indicating a limited effect of the extraction on the volatiles matter contribution. The preexponential factors showed only minor alterations except the last partial peak. Note that the last partial peak is low, wide, and highly overlapped by more prominent peaks. Accordingly, its higher variation may be due to a mathematical ill-definition of its determination, in accordance with the experimental uncertainty values reported by Várhegyi et al. (2004). Since the results include the evaluation of the stepwise experiments, too, they extend the earlier results on the role of extraction and water-washing (Várhegyi et al., 1989b, 2004; Di Blasi et al., 2001a) into a wider domain of experimental conditions.

The situation is more complex in the case of the thistle. The highest alterations were observed at the 2nd and 3rd pseudocomponents. In the case of untreated thistle, a considerable part of the cellulose decomposition occurred in an unusually low temperature domain, and, formally merged into the 2nd pseudocomponent. The water washing diminished this strange behavior, and the obtained partial curves (Panel D1 in Figures 4.3 and 4.4) are similar to those of a regular biomass sample. The data in Table 4.5 reflect this behavior. In the untreated sample c_2 was higher by 0.13 while c_3 was lower by 0.21 than the corresponding values of the water-washed sample. The sum of the c_j coefficients indicates that more char is formed from the untreated sample, in agreement by the higher residue observed during the thermogravimetric

Table 4.5: Summarized Results of the Evaluation using Activation Energies from the Best Kinetic Results for the Washed Samples

			Thistle			Pine[a]			Beech		
			log$A$ (s^{-1})	E (kJ/mol)	c	log$A$ (s^{-1})	E (kJ/mol)	c	log$A$ (s^{-1})	E (kJ/mol)	c
1st pseudo.	Parameters	washed	7.63	101	0.14	11.81	149	0.10	12.16	153	0.12
	Differences[b]	extracted	0.15		0.01	0.02		0.01	0.03		0.01
		washed&ext.	-0.08		0.02	0.06		-0.01	0.03		0.01
		untreated	0.24		0.00	-0.05		0.01	0.03		0.01
2nd pseudo.	Parameters	washed	9.57	130	0.15	14.43	186	0.11	14.21	183	0.09
	Differences	extracted	-0.05		0.10	0.03		0.01	0.02		0.02
		washed&ext.	-0.27		0.03	0.03		0.01	-0.11		0.02
		untreated	0.00		0.13	-0.07		0.00	0.02		0.01
3rd pseudo.	Parameters	washed	13.34	184	0.33	13.53	190	0.50	13.04	185	0.53
	Differences	extracted	0.29		-0.17	0.11		-0.04	0.05		-0.01
		washed&ext.	-0.04		-0.07	0.01		0.00	-0.09		0.01
		untreated	0.23		-0.21	0.07		-0.06	0.11		-0.04
4th pseudo.	Parameters	washed	7.72	130	0.14	16.18	244	0.07	20.89	307	0.05
	Differences	extracted	0.16		0.00	-0.01		0.00	0.27		0.00
		washed&ext.	-0.09		-0.02	-0.55		0.00	0.01		-0.01
		untreated	0.26		0.03	0.10		0.01	0.25		0.00
Fit (%)	Value	washed	1.43			3.04			3.83		
	Difference[c]	untreated	0.21			0.21			0.21		

[a] The initial partial process for the untreated pine sample is not reported in this table.
[b] Alterations from the parameters of the corresponding washed sample.
[c] Alterations from the fit value of the prior best kinetic evaluation.

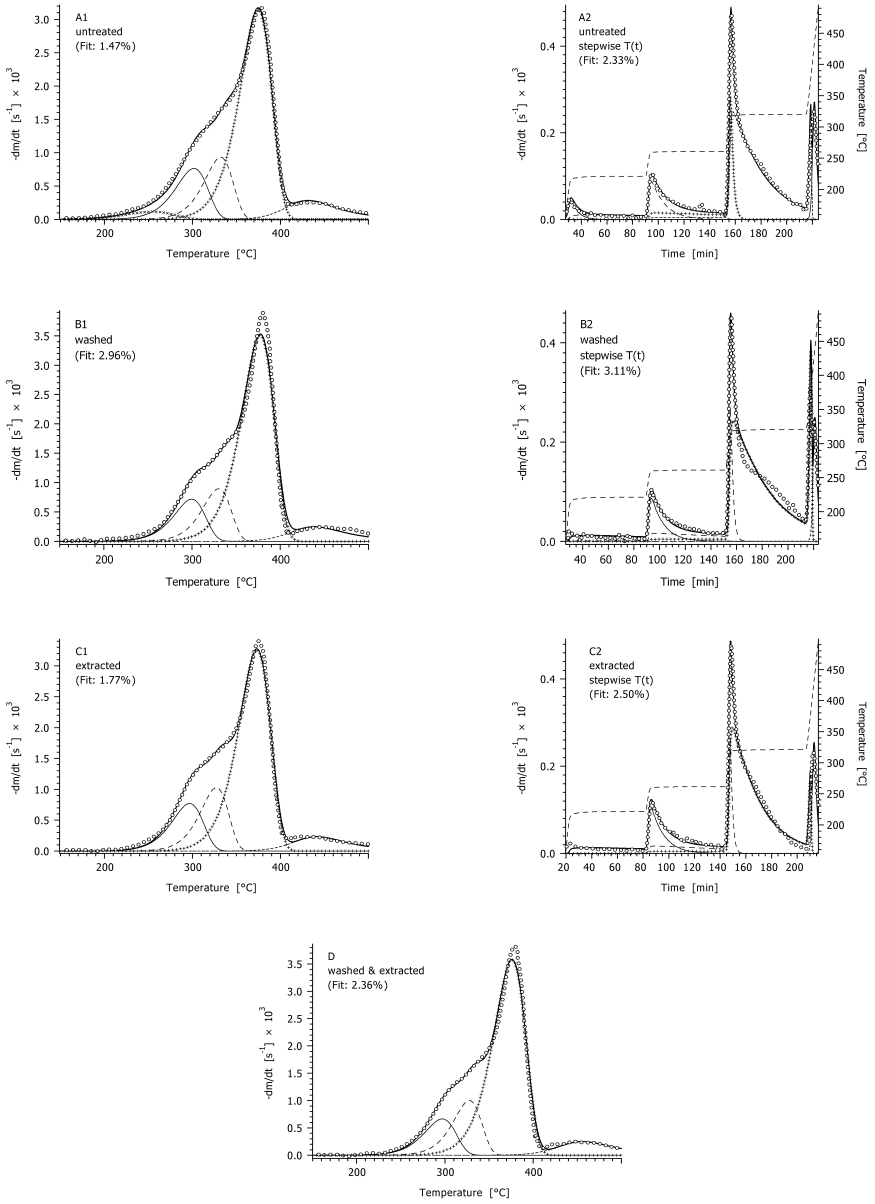

Figure 4.6: Comparison between the observed (o o o) and simulated (—) DTG curves for pine at 20 °C/min (1) and at a stepwise temperature program (line - - - in panel 2) in the Setaram thermobalance, employing third-order reaction for the last pseudo-component and the same E value for all the cases.

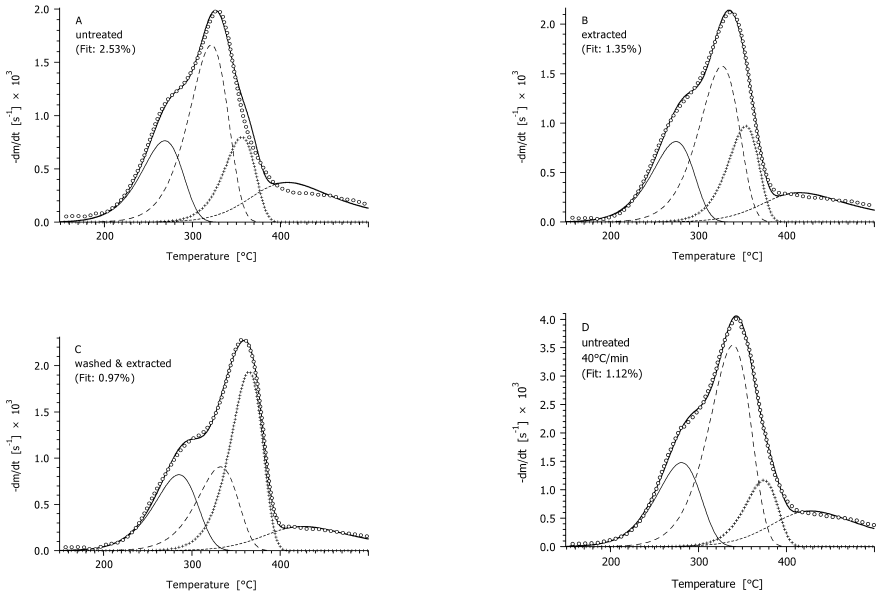

Figure 4.7: Comparison between the observed (o o o) and simulated (—) DTG curves for thistle at 20 °C/min (A -C) and at 40 °C/min (D) in the Setaram thermobalance, employing third-order reaction for the last pseudocomponent and the same E value for all the cases.

experiments. It may be interesting to observe that the magnitude of the 1st and last partial peaks had only minor changes while the corresponding log A values had considerable alterations. The c_j values and the considerations above suggest that the change in the char yield can be connected mainly to the changes in the cellulose decomposition, in the same way as in the woody samples.

Entire set of experiments

Having available experiments from different sources, we were interested in observing how the current kinetic approach predicts the behavior of the samples under equivalent experimental conditions in the different employed thermoanalyzers. In the chapter before we noticed a significant effect of the TGA apparatus on the thermal behavior of the samples. Consequently, we wanted to test the strength of the current approach characterizing the differences between the instruments.

For a given type of sample, experimental results from different apparatus were evaluated simultaneously. On the basis of the latter results with the Setaram thermobalance, the activation energies were taken constant and equal to the set of values coming from the stepwise and the 20 °C/min water-washed experiments (E in table 4.5). The preexponential factors were allowed to vary while the c_j coefficients were kept identical for the different sources. With this approach, we assume that the use of various equipments results in differences mainly in the position of the peaks, and not in their shapes.

The present results are illustrated by Figures 4.8 and 4.9. Observe that the shape of the simulated curves approximates quite satisfactorily with experimental data, even in the case of the Cahn thermoanalyzer, the one with the most sparse data[3] (see panels A2 and B2 in Figure 4.8 and panels D1 and F1 in Figure 4.9). In Tables 4.6 and 4.7, the obtained kinetic parameters are reported as the average of the results from the different equipments for a given type of sample, with variations represented by standard deviations. The temperature peaks ($T_{peak,j}$) corresponding to the simulated partial reactions are also presented. Fits in the tables are the root-mean-square values of the corresponding experiments from different sources, as defined by equation 4.5. The obtained differences in log A and c_j parameters respect to the results in the Setaram thermobalance (diff. in Tables 4.6 and 4.7) are also reported. Due to the repetition of several experiments, each value in the Tables was deduced from 1 - 6 experiments.

Variations in the preexponential factors are easily identified by observing the standard deviations of $T_{peak,j}$. That is to say, a given change in log A is connected to a shift in the peak maxima of the corresponding partial peaks. For the flat, ill-defined peaks (corresponding to the forth partial reactions) the variation is big in most of the cases. The flat peaks describing lignin and further decomposition of the carbohydrate chars proved to be sensitive to the experimental errors in the thermal study of chestnut wood reported by Várhegyi et al. (2004), too, even when the same instrument was used for the repetition of the experiments.

[3]The reader could be addressed to Chapter 3 for a revision of the analysis of the DTG characteristics.

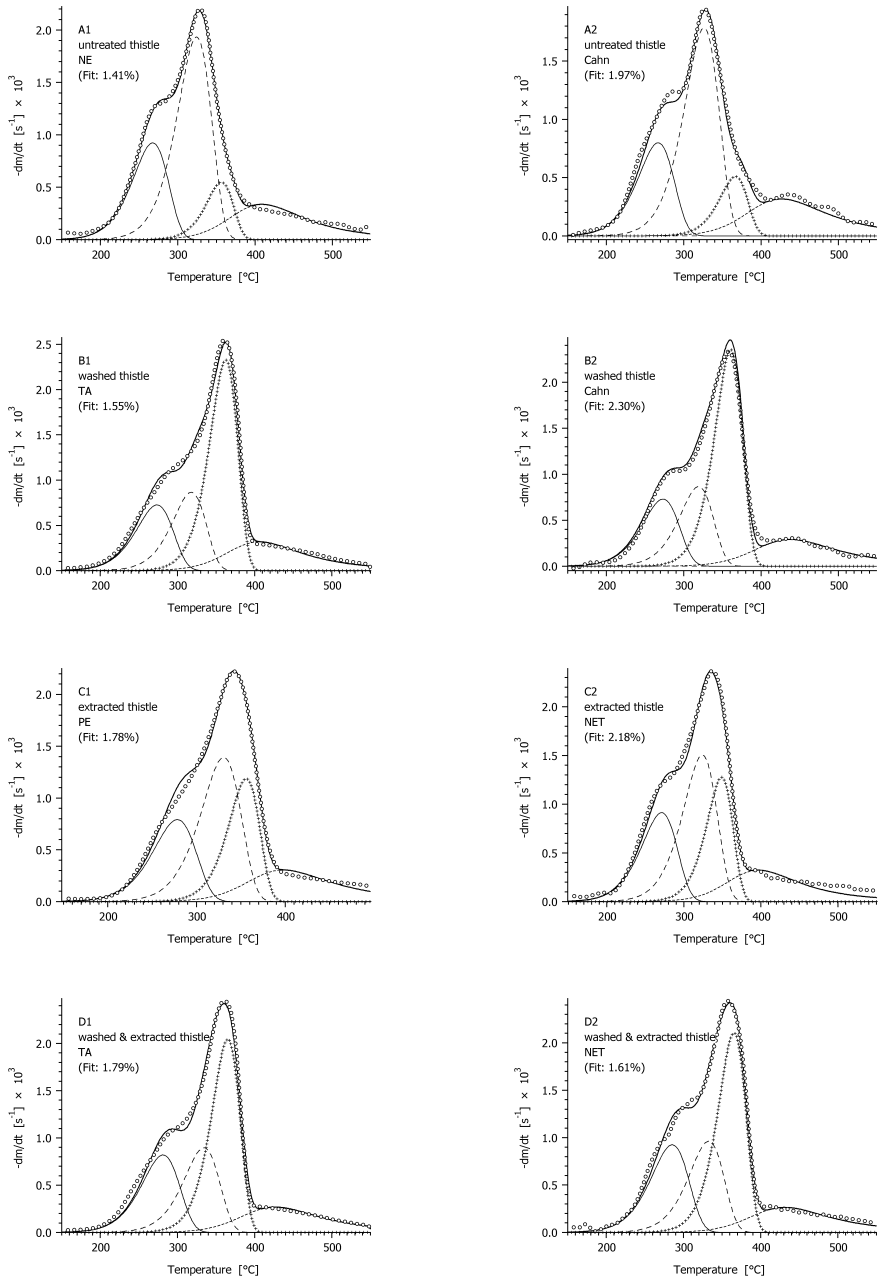

Figure 4.8: Comparison between the observed (o o o) and simulated (—) DTG curves for thistle samples at 20 °C/min in different thermobalances, employing third-order reaction for the last pseudocomponent and the same E value for all the cases (see Table 3.6 for the notation of the thermobalances).

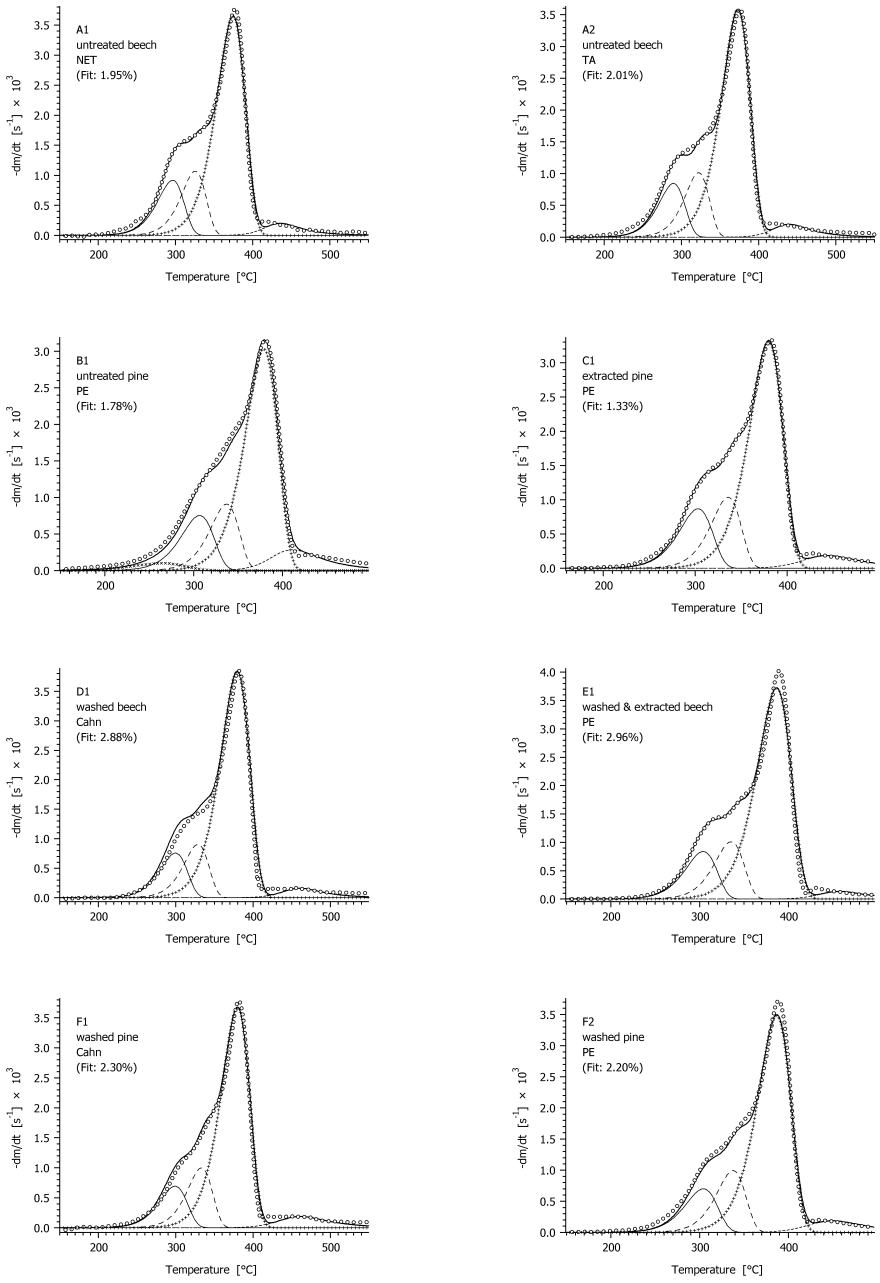

Figure 4.9: Comparison between the observed (o o o) and simulated (—) DTG curves for wood samples at 20 °C/min in different thermobalances, employing third-order reaction for the last pseudocomponent and the same E value for a given type of wood.

Table 4.6: Summarized results of the simultaneous kinetic evaluation of experiments coming from different sources: Thistle

pseudocom.		untreated			washed			extracted			washed&extracted		
		$\log A$ (s^{-1})	T_{peak} (°C)	c	$\log A$ (s^{-1})	T_{peak} (°C)	c	$\log A$ (s^{-1})	T_{peak} (°C)	c	$\log A$ (s^{-1})	T_{peak} (°C)	c
1st	**mean**	**7.85**	**267**	**0.15**	**7.65**	**277**	**0.14**	**7.74**	**273**	**0.14**	**7.52**	**285**	**0.16**
	std. dev.[b]	0.04	**2**		0.09	**5**		0.09	**5**		0.06	**3**	
	diff.[c]	-0.02		0.01	0.03		0.00	-0.03		0.00	-0.02		0.00
2nd	**mean**	**9.47**	**326**	**0.31**	**9.60**	**321**	**0.15**	**9.48**	**327**	**0.24**	**9.32**	**334**	**0.16**
[a]	std. dev.	0.04	**1**		0.07	**4**		0.05	**3**		0.03	**2**	
	diff.	-0.10		0.03	0.03		0.00	-0.05		0.00	0.02		-0.01
3rd	**mean**	**13.42**	**362**	**0.07**	**13.35**	**364**	**0.33**	**13.69**	**352**	**0.17**	**13.28**	**367**	**0.29**
	std. dev.	0.17	**7**		0.06	**3**		0.08	**4**		0.06	**2**	
	diff.	-0.15		-0.04	0.01		0.00	0.06		0.00	-0.02		0.03
4th	**mean**	**7.86**	**415**	**0.14**	**7.91**	**420**	**0.14**	**8.14**	**400**	**0.13**	**7.60**	**432**	**0.12**
	std. dev.	0.22	**18**		0.28	**13**		0.05	**3**		0.07	**5**	
	diff.	-0.11		-0.02	0.20		0.00	0.26		0.00	-0.03		0.00
fit (%)		**1.80**			**1.90**			**2.28**			**1.73**		

[a] E parameters are the same as in table 4.5.
[b] Standard deviations with respect the mean values from different sources.
[c] Alterations from the parameters in table 4.5.

Table 4.7: Summarized results of the simultaneous kinetic evaluation of experiments coming from different sources: Wood

pseudocom.		**untreated**			**washed**			**extracted**			**washed&extracted**		
		$\log A$ (s^{-1})	T_{peak} (°C)	c	$\log A$ (s^{-1})	T_{peak} (°C)	c	$\log A$ (s^{-1})	T_{peak} (°C)	c	$\log A$ (s^{-1})	T_{peak} (°C)	c
Pine[a]													
1st	**mean**	**11.73**	**303**	**0.11**	**11.76**	**302**	**0.10**	**11.73**	**303**	**0.12**	**11.68**	**305**	**0.10**
	std. dev.	0.09	**4**		0.12	**3**							
	diff.	-0.02		0.00	-0.05		0.00	-0.10		0.01	-0.19		0.01
2nd	**mean**	**14.19**	**338**	**0.12**	**14.25**	**335**	**0.13**	**14.24**	**336**	**0.13**	**14.17**	**338**	**0.13**
	std. dev.	0.02	**0**		0.06	**2**							
	diff.	-0.18		0.00	-0.18		0.02	-0.21		0.02	-0.28		0.01
3rd	**mean**	**13.49**	**378**	**0.45**	**13.37**	**383**	**0.53**	**13.45**	**380**	**0.49**	**13.28**	**387**	**0.53**
	std. dev.	0.02	**1**		0.10	**3**							
	diff.	-0.11		0.00	-0.16		0.02	-0.19		0.03	-0.26		0.03
4th	**mean**	**16.22**	**435**	**0.07**	**15.68**	**455**	**0.05**	**15.97**	**444**	**0.05**	**15.69**	**455**	**0.05**
	std. dev.	1.22	**23**		0.14	**5**							
	diff.	-0.25		0.00	-0.50		-0.01	-0.20		-0.01	0.06		-0.02
fit (%)		**2.24**			**2.25**			**1.33**			**1.85**		
Beech													
1st	**mean**	**12.31**	**296**	**0.11**	**12.16**	**302**	**0.10**	**12.19**	**301**	**0.11**	**12.13**	**304**	**0.11**
	std. dev.	0.12	**5**		0.06	**3**							
	diff.	0.12		-0.01	0.01		-0.02	-0.09		0.01	-0.11		0.02
2nd	**mean**	**14.29**	**327**	**0.13**	**14.14**	**332**	**0.12**	**14.16**	**331**	**0.13**	**14.03**	**335**	**0.13**
	std. dev.	0.09	**4**		0.09	**3**							
	diff.	0.07		0.03	-0.06		0.03	-0.15		0.01	-0.22		0.01
3rd	**mean**	**13.15**	**376**	**0.52**	**12.94**	**384**	**0.57**	**12.99**	**381**	**0.56**	**12.85**	**387**	**0.58**
	std. dev.	0.06	**3**		0.11	**4**							
	diff.	0.00		0.03	-0.10		0.04	-0.14		0.05	-0.19		0.05
4th	**mean**	**20.83**	**442**	**0.04**	**20.28**	**458**	**0.04**	**20.55**	**449**	**0.03**	**20.29**	**458**	**0.03**
	std. dev.	0.15	**7**		0.08	**2**							
	diff.	-0.32		-0.01	-0.61		-0.01	-0.23		-0.01	-0.24		-0.01
fit (%)		**2.23**			**3.27**			**2.43**			**2.96**		

[a]Averages of the initial partial process for untreated pine: $\log A = 5.94$, $E = 78$, $c = 0.11$.

In the case of thistle, variations in log A for the rest of partial peaks result smaller than the differences observed between the untreated and pretreated samples (compare tables 4.6 and 4.5), while the woody samples, the less affected by the pretreatments, evidence comparable changes (compare tables 4.7 and 4.5). c_j coefficients report only minor variations respect to the values in table 4.5. On the whole, we consider the means in tables 4.6 and 4.7, in addition to the activation energies in table 4.5, as representative of the best-fit kinetic parameters that describe the primary thermal decomposition of the samples in this thesis.

4.3 Conclusions of this chapter

For each type of material studied in this thesis, several related approaches based on the model of pseudocomponents were applied for determining the best kinetic parameters that describe the pyrolytic behaviour, in the regime of slow pyrolysis.

More satisfactory results were obtained when fitting the DTG curves than using their integral versions (TG curves). The DTG fit revealed that the assumption of three partial peaks was not enough for a reliable, good description of the global mass loss rates. Four partial reactions, related to the domains of hemicellulose, cellulose and lignin thermolysis, were necessary for the satisfactory description of linear and stepwise heating experiments, using the same set of kinetic parameters for a given sample. In the case of untreated pine, an additional low temperature partial peak was also included. Its presence may be connected to the high amount of extractives in this sample. The higher number of partial peaks in the latter evaluation may be due to the involvement of the stepwise heating programs, allowing the accumulation of kinetic information about the chemical heterogeneity of the samples, in a wider domain of experimental conditions.

Previous works based on linear temperature programs established that the assumption of 3rd order kinetics for the high temperature phenomena, dominated by the decomposition of lignin and the further reactions of the residues from the hemicellulose and cellulose, give a better overall fit. The present work extended this result to the simultaneous evaluation of linear and stepwise heating programs. In a test on the thistle sample we got good results for predicting the behavior of high heating rate experiments from the obtained kinetic parameters.

The analysis of the various pretreatment effects was included in a further approximation. We applied the same set of activation energies in the kinetic evaluation of the pretreated and the untreated behaviors of a given sample with varying preexponential factors and c_j coefficients. This approach helped in characterizing the pretreatment effects by quantitative terms. The data obtained in this way showed that the increased volatilization in the water-washed samples is due to the cellulose component. The results revealed a peculiar behavior of the cellulose component in the thistle sample. Water-washing proved to be an effective pretreatment for the deconvolution of the partial reactions in the kinetic analysis.

The latter set of activation energies was also used in the simultaneous kinetic evaluation of the experiments coming from different apparatus, under equivalent ex-

perimental conditions. In this case, only the preexponential factors were allowed to vary. This approach provided a satisfactory description of the global mass loss rates, with quantitatively characterizing the extent of systematic errors by the variations in the position of the peaks. Differences owing to the use of various equipments were well into the range of changes produced by the pretreatments, and similar to those associated with the repeatability of experiments in a same instrument, observed by other authors.

In general, this work showed that the evaluation of the highly overlapped peaks is an ill-conditioned task from single experiments. Instead, unified devolatilization mechanisms for sets of related experiments resulted in good approaches. The work also demonstrated that the assumed reaction kinetics is not only suitable to describe the dynamics of a given sample in a particular experimental case; it is also capable to reveal the actual changes in the samples in a wider range of operational conditions.

Chapter

FIVE

Product distribution from primary biomass pyrolysis

The pyrolytic behavior of biomass materials is not only reflected by the specific weight loss of the samples upon heating, but by the evolution of the different product species, as well. The present chapter extends the current investigations by monitoring the evolution profiles of characteristic pyrolysis products. Mass spectrometry, simultaneously coupled to a thermogravimetric equipment (TG/MS), is used as the volatile product analysis technique. The effect of the pretreatments considered in this thesis (hot-water washing, ethanol extraction and their combination) is also studied. Principal component analysis (PCA) is employed to help in the evaluation of the large data set of results[1]. Making use of calibration data, we estimate the individual production of the major gas species from slow pyrolysis. Then, an approximation of the vapor-phase product distribution is added to the latest kinetic mechanism applied in the chapter before. Sections 5.1 - 5.3 are part of paper A.1.2[2].

5.1 Experimental Section

Equipment

The TG/MS experiments were performed in the Institute of Materials and Environmental Chemistry of the Hungarian Academy of Sciences. The Perkin-Elmer TGS-2 thermobalance (see Section 3.2.4 for the technical specifications of this instrument and the experimental conditions applied) was connected to a Hiden HAL quadrupole mass spectrometer. Prior to the experiments, the apparatus was purged with the carrier gas (argon) for 45 min. A portion of the volatiles formed as a result of thermal decomposition was led through a heated capillary transfer line to the ion source of the mass spectrometer. It should be noted that the relatively low molecular weight products were detected, since the tar fraction was condensed in the apparatus. The mass

[1] The reader should be addressed to Appendix B and Chapter 3 for a revision of the theory, references and applications related to Principal Component Analysis.

[2] Gómez, C. J., Mészáros, E., Jakab, E., Velo, E., Puigjaner, L., 2006.

spectrometer was operated in electron impact ionization mode with 70 eV electron energy. The ion intensities were normalized to the sample mass and to the intensity of the ^{38}Ar isotope of the carrier gas. Corrections of the m/z 16, 28 ions were performed: the corresponding fragment ions of the main decomposition products (water, carbon monoxide and carbon dioxide) were subtracted (Mészáros et al., 2004a).

Calibration data

The mass spectrometric signals were calibrated by the regular procedures of the Hungarian Institute. The amounts of H_2O, CO, and CO_2 were determined by calibration factors calculated from calcium oxalate experiments with the TG/MS arrangement explained above. The reliability of the procedure employed is illustrated by Figure 5.1, which shows the TG, DTG and mass spectrometric ion intensity curves during the thermal decomposition of about 2 mg calcium oxalate monohydrate. The first, second, and third peaks belong to the evolution of water, carbon monoxide, and carbon dioxide, respectively. Ca-oxalate monohydrate evolves crystalline water in the first step, and then CO is eliminated. The third step is the thermal decomposition of the calcium carbonate (Székely et al., 1987):

$$CaC_2O_4.H_2O \longrightarrow CaC_2O_4 + H_2O \tag{5.1}$$

$$CaC_2O_4 \longrightarrow CaCO_3 + CO \tag{5.2}$$

$$CaCO_3 \longrightarrow CaO + CO_2 \tag{5.3}$$

The good fit between the DTG curves and the mass spectrometric intensities established the reliability of both the weight loss and mass spectrometric measurements.

PCA analysis

The integrated intensities of the most significant mass spectrometric fragment ions were considered in the calculations. We selected various data sets with the idea to study the specific influence of the variables, type of sample and pretreatment, on the thermal decomposition and on the product distribution. The MS ion intensities, with good signal/noise ratios, were integrated within the temperature range of decomposition. The m/z ratios of selected products are listed in Table 5.1. The identification of the mass spectrometric ions is based on literature data and on chemical consideration of the wood structure (Faix et al., 1990b,a, 1991b,a; Evans and Milne, 1987; Mészáros et al., 2004a; Pouwels et al., 1987; Pappa et al., 2003; Várhegyi et al., 1988b). MATLAB 7.0 was used as the programming tool for the PCA analysis.

Table 5.1: Selected m/z ratios in the PCA calculations

ion, m/z	Formula	Likely product
2	H_2	hydrogen
15	CH_3^+	fragment of methane and other organic compounds
16	CH_4	methane
18	H_2O	water
28	CO	carbon monoxide
	$C_2H_4^+$	fragment ion of oxygen-containing molecules and hydrocarbons
29	$C_2H_5^+$	alkane and alkene fragment ion
	CHO^+	fragment of aldehydes
30	HCHO	formaldehyde
31	CH_3O^+	main fragment ion of hydroxyacetaldehyde or methanol
41	$C_3H_5^+$	aliphatic fragments
43	CH_3CO^+	fragment of aldehydes, ketones, and other low molecular weight carbonyl compounds
44	CO_2	carbon dioxide
45	$COOH^+$	fragment of acid products
55	CH_2CHCO^+	diverse ion fragmentation (carbonyl compounds, reduced furans, pyranone and phenol derivatives)
57	$CH_3CH_2CO^+$	diverse ion fragmentation (carbonyl compounds, reduced furans, pyranone derivatives and levoglucosan)
58	$CH_3COCH_3^+$	acetone
60	CH_3COOH	acetic acid
	$HOCH_2CHO$	hydroxyacetaldehyde
84	$C_4H_4O_2^+$	furanone

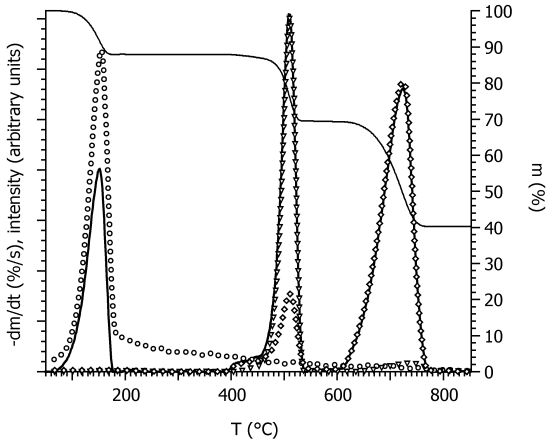

Figure 5.1: Thermal decomposition of 2 mg $CaC_2O_4.H_2O$ at 20°C/min. Symbols represent the MS intensities (o o o: m/z 18, ∇ ∇: m/z 28, $\diamond$ $\diamond$: m/z 44).

5.2 Analysis of the product evolution profiles monitored by mass spectrometry

5.2.1 Comparison of the three different biomass samples

We recorded the evolution profiles of volatile products by mass spectrometry in order to gain insight into the chemical phenomena that accounts for the differences observed among the samples. The TG/MS system could not detect some of the tar fractions (with boiling points above about 180 °C) evolved during the thermal decomposition, due to condensation. However, the evolution profiles of the low molecular mass compounds, produced at low heating rate, characterize the thermal decomposition of the polymeric wood constituents (Jakab et al., 1995; Evans and Milne, 1987; Várhegyi et al., 1988b). The evolution profiles of some selected products of the untreated samples are shown in Figure 5.2. Since the MS intensities of various products have different magnitudes, they have been scaled to obtain comparable peak heights in the plots. For the three biomasses, the scaling factors for the individual species are the same. Accordingly, the intensity of a given product can be compared between the different samples.

As figures 5.2A-C imply, a relatively large amount of H_2O (m/z 18), CO (m/z 28), and CO_2 (m/z 44) is formed from all samples owing to the large number of hydroxyl groups and oxygen atoms present in the natural polymers that make up the cell walls (cellulose, hemicellulose and lignin). The H_2O evolution profile is similar for all the samples. It occurs over the entire temperature range of biomass decomposition, indicating the multiple origin of water. The release of adsorbed water accounts for the peak at around 100 °C, whereas the main peak above 200 °C corresponds to

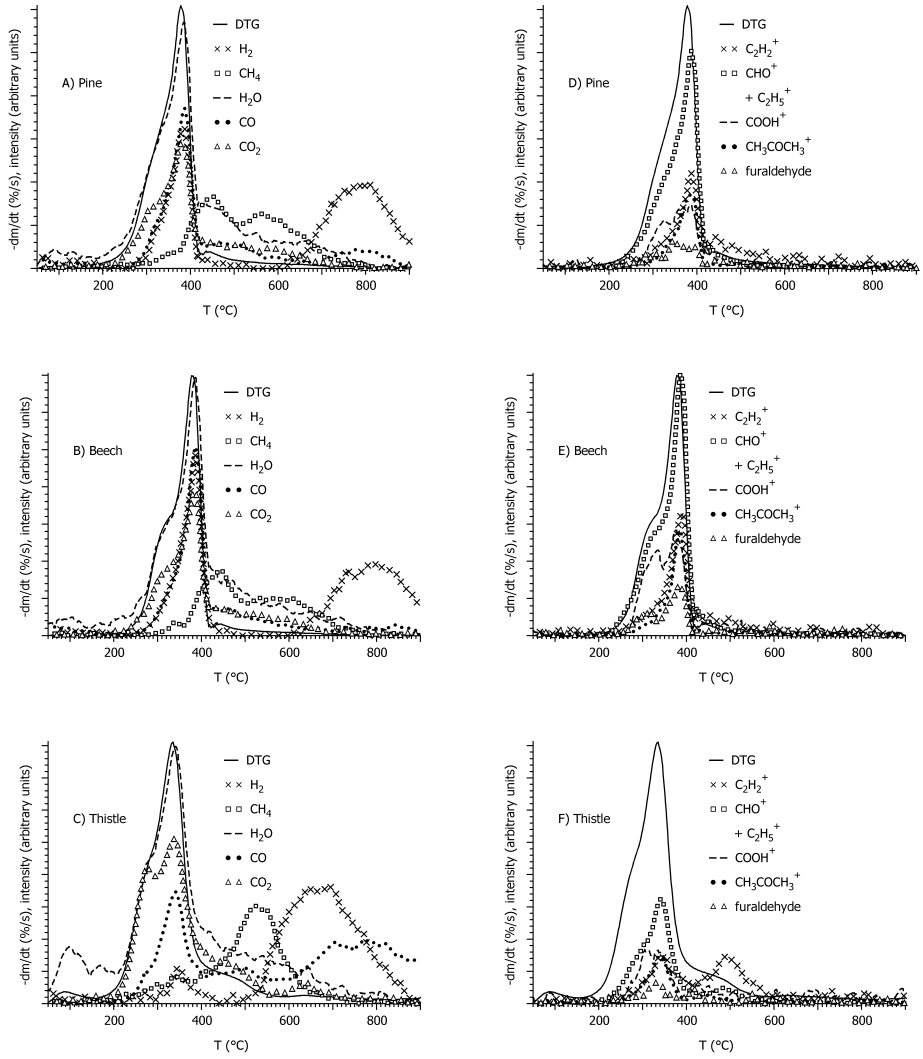

Figure 5.2: The DTG curves and the evolution profiles of some fragment ions of volatile products released from the untreated samples of wood and thistle biomasses.

the water formed in the decomposition of the polymeric cell wall constituents. CO and CO_2 are also formed from cellulose, hemicellulose and lignin. It should be noted that m/z 28 can be the fragment ion of various oxygen-containing molecules (e.g., formaldehyde) and hydrocarbons (e.g., ethane, ethylene). However, the intensity of m/z 28 is much higher than that of the other MS peaks of these products. Therefore, the most significant portion of m/z 28 can be attributed to CO. The MS curves of carbon monoxide and carbon dioxide are different for the given samples above 430 °C. Smaller amounts of CO_2 and CO are formed at around 500 °C from the thistle, and there is also a noticeable evolution of the latter product between 600 and 700 °C. The broad curve of CO above 600 °C can be attributed to the char formation reactions, in which the residual O-functional groups are cleaved.

In the wood samples the m/z 16 profile exhibits two visible maxima at around 440 and 570°C, corresponding to the main processes of methane production. The first process can mostly be attributed to the decomposition of lignin methoxyl groups (Jakab et al., 1997). The methane evolution at higher temperatures corresponds to charring processes. From comparison between the methane curves of wood species and thistle, it can be concluded that the charring reactions play a more significant role in the case of the herbaceous crop, as expected. This result is also confirmed by the more pronounced hydrogen evolution (m/z 2) from thistle in the 500 - 900 °C temperature range, as hydrogen production increases with increasing char formation.

Figures 5.2D-F show the MS curves of some characteristic organic volatile fragments of biomass decomposition. The $COOH^+$ (m/z 45) ion is a characteristic fragment of the decomposition of both cellulose and hemicellulose. The acetylate side groups of xylan polymer can explain the noticeable amount of acid products released at the hemicellulose devolatilization domain, whereas acetone (m/z 58) originates mostly from cellulose. The m/z 96 product represents furaldehyde. It is interesting to note that in the case of wood samples the more discernible shoulder on the DTG curve at around 320 °C is also observable in the MS profiles of all those distinctive products of polysaccharide decomposition. It implies that the thermal decomposition of hemicellulose and cellulose is less overlapped in the wood samples.

The amount of volatiles produced from polysaccharides is expected to be considerably higher than the organic evolution from lignin (Evans and Milne, 1987; Mészáros et al., 2004a). In our case the thistle sample, with the highest lignin content, evolves the lowest yield of some of the organic products, e.g. acetone and acetic acid. On the other hand, beech, the sample which evidenced the maximum rate of decomposition, shows correspondingly the largest peaks.

Some other ionization fragment ions were also monitored. The peak of $C_2H_2^+$ (m/z 26) and $C_2H_5^+$ (m/z 29) can be representatives of alkane and alkene fragment ions, although m/z 29 can also be a fragment of aldehydes (CHO^+). It is interesting to note that both fragments ions are detected in the main decomposition process and at around 480 °C from the thistle sample, whereas these products only occur in the region of cellulose decomposition in the case of the wood species. The origin of the peak occurring at 480 °C from the thistle may be the presence of extractives in the herbaceous crop.